STUDY OF THE IMIDIZATION OF POLYAMIC ACID USING MICRODIELECTROMETRY

A THESIS

Presented to

The Faculty of the Division of Graduate Studies

By

Hemant Nanavati

In Partial Fulfillment

of the Requirements for the Degree

Master of Science in Chemical Engineering

Georgia Institute of Technology

March, 1992

STUDY OF THE IMIDIZATION OF POLYAMIC ACID USING MICRODIELECTROMETRY

Approved:

Sue Ann Bidstrup, Chairman

A. S. Abhiraman

Paul A. Kohl

March 5, 1992

Date Approved by Chairman

ACKNOWLEDGEMENTS

A number of people have contributed to this work and helped me see it through completion. I'm in their debt. I'm especially grateful to my advisor, Dr. Sue Ann Bidstrup who gave me the opportunity to pursue research in this area. Dr. Bidstrup also provided the guidance and support without which this thesis would not have been possible. She devoted extra time and energy and effort to ensure that in spite of myself, this thesis reflected my best effort. For this too I'm grateful.

I would like to extend my sincere appreciation to the Dr. A. S. Abhiraman and Dr. Paul Kohl for serving on my Reading Committee. Their advice and suggestions were very helpful in developing this work. Sincere thanks to Dr. Abhiraman for the moral support he gave me and his concern.

Materials donation from E. I. Du Pont de Nemours and Company (Inc.), Electronics Division and financial support from Manufacturing Research Center at Georgia Tech and the Presidential Young Investigator Program of the National Science Foundation is gratefully acknowledged.

Special thanks are extended to my group-mates and friends- Jim Companik, Linda Lin and Joycelyn Simpson. Your contributions from the brainstorming sessions, personal moral support and cooperation have been invaluable. I'm especially indebted to my office-mate Linda Lin. She has always been there (being available at ungodly hours to prepare the samples for FTIR spectroscopy being one of the many cases in point). Her friendship has been a privilege. Special thanks also to Linda Lin and office-mate and friend Tom Hodge for assistance in proof reading this thesis.

I would like to take this opportunity to thank Steve Hardaker for training me to use the FTIR Spectrometer and helping me learn to interpret spectroscopy data.

Life in the USA has been a wonderful experience. I'll always treasure the many friendships I've made in my two and a half year stay. Like I always tell the new Indian students before they find out for themselves - the natives are a very friendly bunch. Numerous special friendships have developed within the Indian community also during the course of this phase of my pursuit of graduate study and have made my stay here quite enjoyable: Rangaswamy Rajamanickam (Ranga), Nilesh Shroff, Pankaj Upadhyay, Ram Kumar Ramesh (Ravan), Vishnu Vandana, Anuradha Khawas (Anu), Bodhisattwa Mukherjee (Bodhi), Arun Mangalam (Sac - old friend and new too), the Dalal family (Satishbhai, Smitaben, Tanvi and Nija).

I extend my sincere gratitude to my parents, Jayantkumar and Uma Nanavati, my brother, Kaushik Nanavati, my late uncle, Vasantlal Nanavati and my grandmothers, Navnitben Nanavati and Nirmala Khandwala for their continued love and moral support from across the seven seas.

You are all priceless jewels in the treasury of my life.

TABLE OF CONTENTS

LIST OF TABLES

LIST OF FIGURES

NOMENCLATURE

A_{1370}	absorbance at 1370 cm^{-1}
A_{1500}	absorbance at 1500 cm^{-1}
$A_{T_i}^{\nu}$	absorbance at wave number ν and temperature T_i.
c	velocity of light (3×10^8 m/s)
$\overline{\cos\ \gamma_{1j}}$	value of the $\cos\gamma_{1j}$, averaged over the entire chain.
$\overline{^{I}\cos\ \gamma_{1j}}$	average of the cosine of the angle between a reference unit 1 and a unit j within the same polymer chain. This term corresponds to intra-chain interactions.
$\overline{^{II}\cos\ \gamma_{ij}}$	average of the cosine of the angle made between a reference unit i and a unit j which does not belong to the polymer chain that contains the reference unit i. This term corresponds to inter-chain interactions.
D	displacement vector of charged species
D(t)	displacement of charged species as a function of time
d	density
$d\omega_1$, $d\omega_2$	surface elements of the solid angles of the directions of the two dipoles.
E	electric field vector
E_0	amplitude of oscillation of the applied sinusoidal electric field
E(t)	electric field as a function of time
f(Hz)	frequency in Hz

$f(\omega)$	frequency dependant part of the complex dielectric constant
FW	formula weight
g	interaction parameter
g'_r	interaction parameter for a repeat unit in a polymer molecule
g'_{r-ij}	interaction parameter for units of species i and j
h	Planck's constant (6.626×10^{-34} J-s)
J	displacement current vector
j	square root of -1
k	Boltzman's constant (1.38×10^{-23} J/mol.°K)
M	molecular weight
m	dipole moment of a point dipole
$\overline{\mathbf{mm}^*}$	average value of the product $\mathbf{mm}^*$ taking into account all the possible configurations and weighing them according to the probability of finding the unit in such a configuration.
$\mathbf{m}^*$	dipole moment of a large spherical region embedded in its own medium polarized by one of its units which is in such a configuration that its dipole moment is **m**
N_m	number of dipoles per unit volume
N_r	Number of monomer repeat units per unit volume
N_{r1}	N_r of the polyamic acid-NMP complex (1.227×10^{27} amic acid units/m^3)
N_{r2}	N_r of the polyimide fraction (2.086×10^{27} imide units/m^3)
P	polarization
P(t)	polarization as a function of time
P_0	initial polarization
$\mathbf{p}_i, \mathbf{p}_j$	dipole moments in the gaseous phase of species i and j

$\mathbf{p}_k$	dipole moment of the k^{th} monomer repeat unit.
$\mathbf{p}_o$	dipole moment of the monomer repeat unit if it could and were to exist in the gaseous phase
S	entropy
S_0	entropy in absence of an applied electric field
T	temperature in °C.
t	time
Tg	glass transition temperature
U	energy of interaction between neighboring molecules
$U_{o\text{-}ij}$	interaction energy between species i and j
x	extent of imidization
x_i, x_j	mole fractions of groups i and j respectively
z	number of nearest neighbors to a molecule or a monomer unit
α_E	deformation polarizability
α	orientation polarizability
β	distribution parameter for relaxation times
γ	angle between two dipoles
γ_{1j}	angle between the reference unit 1 and the j^{th} unit in the same polymer chain.
μ	dipole moment of a molecule
$\langle\mu\rangle$	mean dipole moment of a molecule of a polar gas
μ^*	dipole moment of a large spherical region embedded in its own medium polarized by one of its molecules which is in such a configuration that its dipole moment is μ
μ_0	dipole moment of a molecule in the gaseous phase

ε''	relative loss factor
ε'	relative permittivity
ε^*	complex dielectric constant
ε_R	relaxed relative permittivity
ε_U	unrelaxed relative permittivity
ε_0	permittivity of free space ($10^{-9}/36\pi$ Farad/m)
ν	wave number in cm^{-1}
ω	angular velocity (radians/second)
σ	ionic conductivity ($1/\Omega m$)
τ_d	the mean of dipole relaxation times

SUMMARY

Polyimides have a wide range of applications in the electronics industry. The end uses of the polyimides depend on their dielectric performance which depends on the extent of imidization. Permittivity and loss factor characterize the dielectric performance of a material. Their measurement has been greatly facilitated by the advent of microdielectrometry. This technique has great potential for monitoring the imidization of polyamic acid to polyimide. Most of the traditional methods for determining the extent of the imidization reaction cannot be used for in-situ monitoring. Additionally, they have a very low sensitivity towards the end of the reaction. Therefore, it is more advantageous to use the indirect method of microdielectrometry to obtain structural information. However, in order to utilize microdielectrometry confidently to monitor and control the imidization reaction, it is necessary to relate the dielectric properties to the molecular structure.

Previous microdielectrometric studies on polyimides have been on qualitative monitoring of imidization and moisture diffusion in fully imidized films. In each of these cases, the focus was on the loss factor. The present investigation uses microdielectrometry and FT-IR spectroscopy simultaneously to study the effect of the extent of reaction on the permittivity. In the case of polyimides, the permittivity, as opposed to loss factor has the potential to be related to the molecular structure. In the present research a model to relate the permittivity of the material to the chemistry at various stages of the imidization has been developed.

CHAPTER I

MOTIVATION AND BACKGROUND

1.1 Dielectric Analysis of Polymers used in Microelectronics

Polymers are extensively used as insulating and support materials in microelectronics components. Traditionally, inorganic materials (eg. silicon dioxide and silicon nitride) were used for this purpose because of their high thermal and chemical stabilities which are necessary to withstand the hazardous environment generated in the fabrication processes. Recently, polymers have replaced these materials because they are easier to process.

Polyimides are used as passivation layers and interlevel dielectrics in microelectronic applications. This investigation focuses on the analysis of the imidization of polyamic acid to polyimide using dielectrometry. Dielectric properties change drastically during imidization. Understanding this change is crucial for designing optimum processing schedules and for process control. Recent technological advances have made it possible to fabricate dielectric microsensors directly on the surface of a silicon wafer. If the relationship between the extent of imidization and dielectric properties could be established, then these dielectric microsensors could be used to characterize the imidization reaction.

Several researchers have monitored and modelled changes in dielectric properties for reacting polymer systems {[Senturia and Sheppard, 1986], [Bidstrup, W.W. et al. 1988], [Kranbuehl et al. 1982, 1988], [Bidstrup, S. A. , Sheppard and Senturia, 1989], [Day, 1989], [Nass and Seferis, 1989]}. This work has been largely on reactions of thermosetting polymers, although Day and Senturia (1982) have studied changes in dielectric properties during imidization for thermoplastic polyimides. However, the present investigation is novel in that it measures the dielectric permittivity as a function of the chemistry. This chemistry is independently determined under conditions identical to the dielectric measurements. The purpose is to be able to use the relative permittivity to predict the molecular structure by determining the dipole moment of the basic unit of the material and thus determine the extent of the reaction.

1.2 Importance of Polyimides in Microelectronics

1.2-1 Applications of Polyimides in Microelectronics.

Microelectronic circuits are made up of layers of complex patterns of micron size conducting lines made of aluminium, silver, gold copper and their alloys. Adjacent metal layers are insulated from each other by layers of interlevel dielectrics sandwiched between them [Sze, 1983]. The topmost or passivation layer of the integrated circuit (IC) insulates the circuitry from attacks by corrosive species like moisture and ionic contaminants. These insulators or dielectrics were traditionally made up of ceramic materials.

Technological advances in the integrated circuit fabrication industry have made the circuits denser and more complex, and the circuit components smaller. The inorganic

dielectrics reproduce the topology of the underlying conducting substrate, thus making it more difficult to introduce subsequent conducting layers. Organic polymers, having superior planarizability, are therefore used as interlevel dielectrics.

Polyimides are among the most commonly used polymers in the microelectronics fabrication industry. They are used as plastic insulation materials, passivation layers and photoresists. In IC packaging, they are used as a particle barriers, die attach material, film carrier, thick film paste, dielectric for hybrid circuits and multi-chip modules, PCB dielectric, encapsulant for packaging and as a junction coating for discretes [Soane and Martynenko, 1989]. Polyimides are also used as masks in the ion-implantation process, as mask substrates in the x-ray lithography process, and as a lift-off stencil in photolithography. However, the major focus has been in the application of polyimides as interlevel dielectrics to facilitate greater circuit density for semiconductor devices.

1.2-2 Monitoring Extent of Imidization

In a typical IC fabrication process, a solution of polyamic acid, which consists of the polyimide precursor dissolved in a highly polar solvent like n-methyl pyrrolidinone (NMP), is dispensed on the silicon wafer. The polyamic acid solution is then spin-coated by rotating the wafer at speeds of the order of 5000 rpm for about thirty to sixty seconds. Thus, a uniform coating is obtained. A prebake is carried out to evaporate most of the solvent. The prebake is followed by a high temperature treatment of the material.

In this imidization step, changes take place in the molecular structure due to the cyclodehydration reaction. A covalent bond is formed by a ring closure. This involves dehydration and release of bound solvent. These chemical changes cause drastic changes in the mechanical and electrical properties due to the rigidification of the structure. The

chemical stability and solvent resistance increase due to the removal of the reactive sites. Also, mechanical strength increases due to the formation of a rigid imide ring.

The imidization reaction has been studied using numerous techniques. These include dynamic mechanical thermal analysis (DMTA) [Feger, 1987], FT-IR spectroscopy {[Pryde, 1989-a], [Osredkar, 1988], [Snyder and Painter, 1989]}, thermogravimetric analysis (TGA) [Wilson et al., 1982], differential scanning calorimetry (DSC) [Wilson et al., 1982], [Navarre, 1982], fluorescence spectroscopy [Wachsman and Frank, 1988], and dielectrometry{[Day and Senturia, 1982], [Kranbuehl et al., 1982]}, chronogravimetric analysis [Wilson et al., 1982], mass spectrometry [Soane and Martynenko, 1989] and degree of film dissolution with solvent treatment [Soane and Martynenko, 1989]. This investigation will concentrate on the combined use of dielectric and FT-IR spectroscopic analyses to correlate the structural changes during imidization to changes in the dielectric properties.

1.3 Structure - Property Relationships

The end use of a material depends on its performance properties. These performance properties depend largely on molecular structure. Polymers offer a significant potential for application as dielectrics in the semiconductor industry. To be actually used in this application the organic polymers need to withstand the hazards of the environment of microelectronics fabrication and meet the performance property standards set by the inorganic dielectrics used previously. These requirements include, among others, minimal outgassing of residual solvent or moisture, stability up to 400°C without volatile by-products, and a glass transition temperature higher than the highest temperature of the

subsequent IC processing temperatures (200-400°C). These material properties have been translated into their structural requirements in Table 1.1. [After Soane and Martynenko]

Polyimides have excellent planarizability because their prepolymers are available in solution form. Their application as thin films reduces the effect of the resistance to the diffusion of volatiles, thus leaving no micropores. This can be seen from their excellent mechanical properties {[Wilson, 1981], [Du Pont Company, 1988]}. Polyimides have very good thermal stability to withstand the large variations in temperature [Jensen and Lai, 1989] that take place during the processing. Polyimides have very good chemical stability

Table1.1 : Criteria for the design of an organic polymer as a dielectric.

Desired Property	Structural Requirement
Planarizability	• Low Molecular Weight Prepolymer (melt before cure) or Prepolymer available in solution form.
No Microporosity	• Cured by Addition Reaction or Polymer used is a thin film to facilitate diffusion of evolved volatiles.
Thermal Stability	• Incorporate Aromatic Units
No Moisture Pick-up	• Eliminate H_2O Adsorbing Groups
Low Dielectric Constant	• Eliminate Polar Groups
Lithographic Sensitivity	• Photosensitive Prepolymer
High Mechanical Properties	• Optimize Contour Length (crosslinks)

and are resistant to the chemicals used during the IC fabrication process {[Soane and Martynenko, 1989], [Tessier et al., 1989]}, though moisture absorption of polyimides is a concern for their application in IC circuits. The dielectric properties of polyimides are

comparable to those of previously used inorganic materials {[Brown, 1982], [Soane and Martynenko, 1989]}. There is a long-term reliability concern due to the stress buildup [Geldermans et al., 1982] caused by the mismatch of the coefficient of thermal expansion (CTE) between the polyimide and the adjacent layers.

Molecular structure strongly affects mechanical properties (i.e. modulus), transport properties (i.e. diffusivity and viscosity), chemical properties (i.e. stability and solvent resistance), dielectric properties (i.e. permittivity and bulk conductivity). Hence, it is necessary and of paramount importance to understand the physical relationship between molecular structure and the corresponding performance properties.

1.4 Motivation and Research Goals

One of the reasons why polyimides are used as interlevel dielectrics is their favorable dielectric properties. Since these dielectric properties are crucial to their final application, the idea of using changes in these properties to predict change in chemical structure due to imidization is particularly interesting.

Dielectric properties were first reported to be used as a measure of extent of reaction by Kienle and Race in 1934. Major advances have been made since for measuring dielectric properties for reactive polymer systems{[Senturia and Sheppard, 1986], [Bidstrup, W.W. et al. 1988], [Day and Senturia,1982], [Kranbuehl et al. 1982, 1988], [Bidstrup, S. A. , Sheppard and Senturia, 1989], [Day, 1989], [Nass and Seferis, 1989]}.

During imidization, the material undergoes large changes in properties and structure. These changes, as mentioned earlier, include increases in viscosity, modulus, glass transition temperature, chemical stability and thermal stability. More importantly,

there is also a drastic decrease in dielectric properties. Various methods can be used for monitoring extent of reaction including dynamic mechanical thermal analysis (DMTA), TGA and FT-IR spectroscopy. FT-IR spectroscopy has the disadvantage of low sensitivity near complete imidization. Additionally, problems are caused by the overlapping of peaks, sloping baselines and the necessity to obtain a completely imidized sample as a reference against which to ratio the results; it is impossible to obtain a sample that is 100% imidized. However, FT-IR spectroscopy has the advantage of being able to measure chemical change directly. It is critical to have a method that accurately measures the small changes in the extent of imidization *in-situ*, so that one can have instantaneous information on the chemical structure and performance properties. Dielectric properties are among the most significant performance properties for the insulating applications of polyimides, and it would be advantageous to use them to monitor the imidization.

Dielectrometry has several advantages over other techniques of monitoring chemical reactions like imidization and thermoset cures. Dielectric measurements follow the cure reaction to completion and can even follow small changes in chemistry, especially near the end of the reaction. In an earlier study on epoxies [Micromet Instruments, Inc.], thermal measurements ceased to show change after 45 minutes of cure whereas dielectric measurements did not level off until two hours. In addition, microsensors for dielectric measurements have been developed. These probes for the microdielectrometer are themselves silicon integrated circuits and their geometry is ideal for *in-situ* study of thin films intended for microelectronic applications. Hence, there is interest in implementing microdielectrometry to monitor changes in dielectric properties as a function of extent of reaction.

The imidization reaction taking place causes a change in dielectric properties. This is because the chemical structure of the material changes due to the reaction. Hence, before

microdielectrometry can be used as an effective monitor of the imidization reaction, a fundamental and physical understanding of the relationship between the molecular structure and dielectric properties is required. Only then can this method be used for process monitoring and control. The aim of this investigation is to monitor the dielectric properties and the extent of imidization of a material in such a way that the history and environment of the samples undergoing the two analyses are identical. In this manner it will be possible to obtain dielectric properties as a function of the extent of imidization.

This investigation focuses on determining the dielectric properties as a function of the extent of the imidization reaction. Subsequently, a theoretical model to relate the permittivity to the extent of conversion is developed. The method used will be to determine the extent of imidization by FT-IR spectroscopy and the dielectric properties at that instant in the imidization process will be determined by microdielectrometry. Thus, an attempt will be made to develop a method to predict the degree of imidization at any time based on the measured dielectric properties.

1.5 Synopsis

The rest of the report of this investigation is divided as follows:

- In Chapter 2, basic principles of dielectrometry are presented. In addition, polyimide chemistry is discussed and an overview of different methods that have been used to monitor extent of imidization is presented. A brief discussion on previous FT-IR work on polyimides and previous work in dielectrometry is also presented.

- In Chapter 3, the experimental procedure is described for the microdielectrometry and the FT-IR spectroscopy aspects of the investigation. The experimental results are also presented in this chapter.
- In Chapter 4, the development of the theoretical model to relate the permittivity to the extent of imidization is presented. The analyses of the experimental data and the modelling results are also discussed in this chapter.
- In Chapter 5, the summary of this investigation and the scope for future work in this area is discussed.

CHAPTER II

LITERATURE SURVEY

2.1 Dielectrometry

2.1-1 Basic Principles

Dielectrometry is concerned with measuring and characterizing the response of a material to an applied electric field. This electric field is created by placing the material to be studied between two conducting electrodes and applying a sinusoidal voltage across the electrodes. This will cause a displacement of the charged units in the material. If the charged units are dipoles, they will orient in the direction of the field as shown in figure 2.1. If the charged units are mobile (i.e. free electrons or ionic impurities), then conduction will take place as shown in figure 2.2. Usually, both kinds of charges are present in varying amounts. A good dielectric will have very few dipoles and negligible quantities of free, mobile charges.

When the frequency of the applied voltage is very low, a phenomenon known as electrode polarization takes place. There is an accumulation of ions at the electrodes and a heightened orientation of the dipoles. This phenomenon is discussed in section 2.1-3.

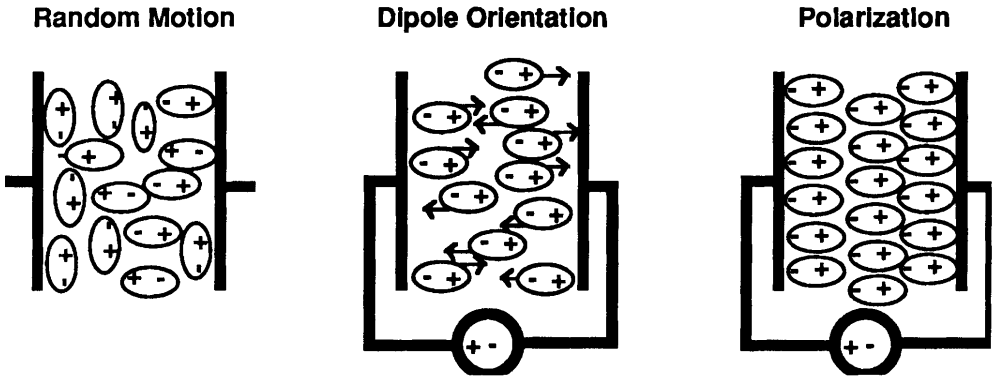

Figure 2.1: Illustration of orientation of dipoles between conducting electrodes in the presence of an applied electric field. (After Senturia, 1986)

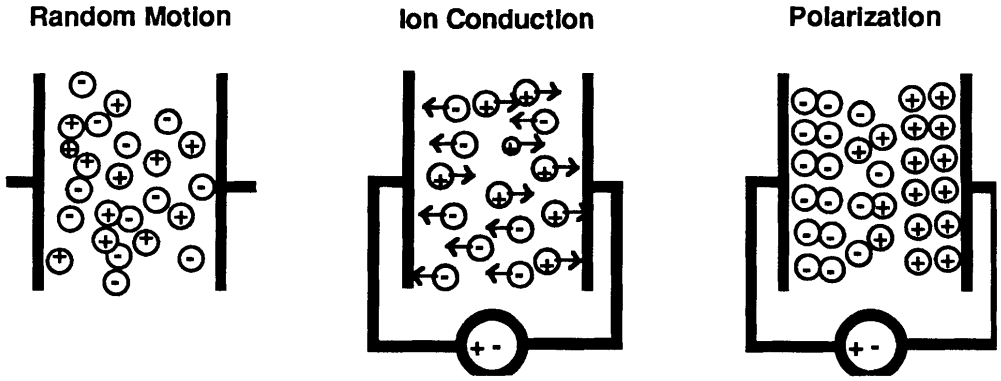

Figure 2.2: Illustration of conduction of ions between conducting electrodes in the presence of an applied electric field (After Senturia, 1986).

The dielectric displacement is directly proportional to the applied electric field. This is derived from Gauss' law of electrostatics.

$$\mathbf{D} = \varepsilon_0 \varepsilon^* \mathbf{E} \qquad (2.1)$$

D and **E** are the displacement and electric field vectors respectively. ε_0 is the permittivity of free space ($10^{-9}/36\pi$ Farad/m). ε^* is the dielectric constant of the material. In general, **D** and **E** can be expressed as complex quantities. Hence, the dielectric constant too can be expressed as a complex quantity.

The electrode geometry is also important. Two of the most commonly used geometries are parallel plate (figure 2.3) and comb electrode (figure 2.4). When using the parallel plate geometry, the sample is kept between the plates and the dielectric properties are measured. This method has the advantage of simplicity in interpreting the measured capacitance and resistance in terms of the dielectric properties of the material. However, it is not advantageous to use this geometry because of the inaccuracies caused by dimensional changes due to temperature changes, pressure and reaction induced shrinkage. There is also the possibility of the creation of voids due to the entrapment between the parallel plates of volatiles that are evolved during the reaction. The comb electrode geometry consists of metal electrodes patterned on an insulating substrate of silicon dioxide or ceramic using photolithography. Its advantages are that its dimensions are precise due to its microelectronic fabrication, and that the material only needs to completely cover the active face of the sensor (~2x3.5mm). Dielectric analysis can be conducted either by using a sensor dipped in the material or placing a single drop of the material on the sensor or by embedding the sensor in the sample or in a piece of the process equipment. The comb electrode geometry is used in this investigation.

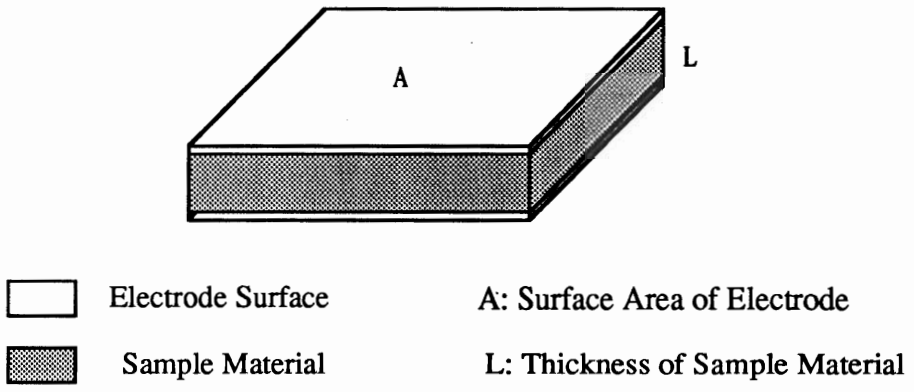

Figure 2.3: Schematic of the parallel plate capacitor geometry.

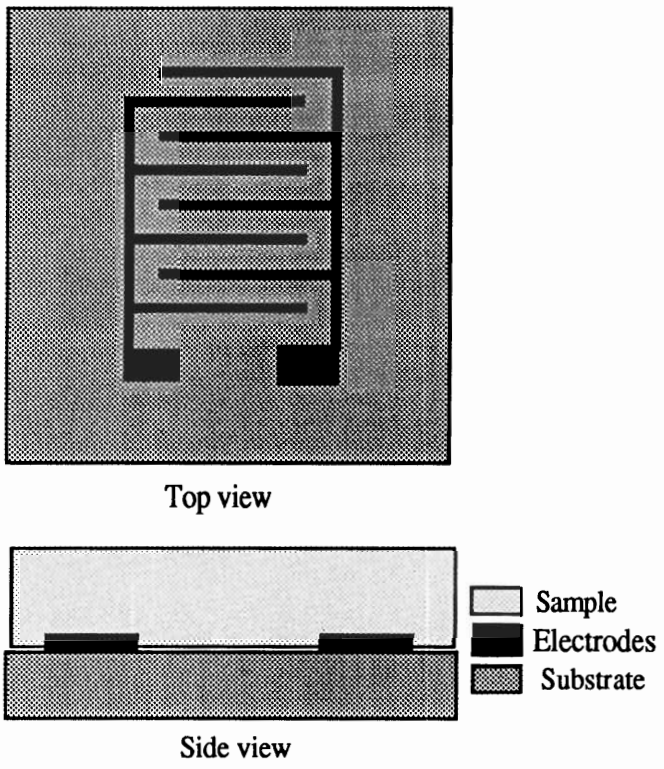

Figure 2.4: Schematic of comb electrode pattern fabricated on the surface of the microsensor

The dielectric measurements are carried out by applying sinusoidal voltages. Assuming ideal electrodes, consider a homogeneous material in a uniform sinusoidal electric field, E(t).

$$E(t) = E_0 \cos \omega t \qquad (2.2)$$

E_0 is the amplitude of the field and ω is the angular velocity. This can be expressed in complex exponential notation as:

$$E(t) = \mathrm{Re} \{ \mathbf{E}\, e^{-j\omega t} \} \qquad (2.3)$$

The displacement, which is proportional to the field, comprises of orientation and conduction of charged species and can be expressed as:

$$D(t) = \mathrm{Re} \{ \mathbf{D}\, e^{-j\omega t} \} \qquad (2.4)$$

E and **D** are the vectors of the field and the displacement respectively, and j is the square root of -1. The displacement current vector **J,** is the time rate of displacement and is hence related to the field as:

$$\mathbf{J} = j\, \omega\, \varepsilon_0 \varepsilon^*\, \mathbf{E} \qquad (2.5)$$

The complex dielectric constant, is a function of the frequency and can be expressed as:

$$\varepsilon^* = \varepsilon'(\omega) - j\, \varepsilon''(\omega) \qquad (2.6)$$

The real part, $\varepsilon'(\omega)$ is the relative permittivity and the imaginary part, $\varepsilon''(\omega)$ is the loss factor.

2.1-2 The Dielectric Constant

The dielectric constant, $\varepsilon^*(\omega)$, of a non-conducting material, is a measure of its polarization due to an electric field. One or more of electronic, atomic, orientational and interfacial polarizations occur, depending on the frequency of the field. Energy is applied in this polarization process in the form of an electric field. During polarization, part of the energy is retained, and the remainder is lost. The relative permittivity is a measure of the energy stored, and the loss factor is the measure of the energy loss during the polarization.

Electronic polarization is the slight displacement of the electrons with respect to the positively charged nucleus. Atomic polarization is the relative displacement of atoms in a polar covalent bond. Orientational polarization is the orientation of the permanent dipoles along the electric field. Interfacial polarization is the accumulation of mobile charges (eg. ions) at the electrodes when the charges are transported through the bulk faster than they are discharged at the electrodes.

The time required for polarization corresponds to the distance over which charge is displaced and the ease of displacement. Electronic and atomic polarizations correspond to very low displacement distances and take place fairly easily. Hence they require very little time. These polarizations are, therefore independent of frequency since only frequencies above 1 GHz affect them and the highest frequency being used in the present investigation is 100 kHz. Interfacial and orientational polarizations take place at much lower frequencies and are therefore taken to be frequency dependent.

Due to the variety in the kinds of possible polarizations, the permittivity can be considered to be made up of two parts - the frequency dependant part and the frequency independent part [Solymar and Walsh, 1988]. The part independent of frequency corresponds to the electronic and atomic polarizations and is called the unrelaxed permittivity. It will be denoted as ε_U. At the other extreme, that is at very low frequencies, all polarizations are complete, and the corresponding permittivity is the relaxed permittivity, ε_R. At any given frequency, the actual permittivity of a material lies somewhere in between these two values. The dipoles are rigidly attached to larger molecules in a viscous medium. Hence, their orientation process has a characteristic time, called the dipole relaxation time and is denoted by τ_d. The hindering mechanism causes losses to be associated with the orientation process. One can express the dielectric constant as:

$$\varepsilon^* = \varepsilon_U + f(\omega) \qquad (2.7)$$

At very low frequencies, ω is close to zero and ε^* is very nearly equal to ε_R. Hence,

$$f(0) = \varepsilon_R - \varepsilon_U \qquad (2.8)$$

If a steady field is applied and then switched off, the polarization P decays exponentially from an initial value of P_0 with τ_d as the time constant.

$$P = P_0 \exp(-t/\tau_d) \qquad (2.9)$$

Taking the inverse Fourier transform to convert to the frequency domain,

$$f(\omega) = K\int_0^{\infty} P(t)\, e^{-j\omega t}\, dt$$

$$= \frac{KP_0\tau_d}{j\omega\tau_d + 1} \qquad (2.10)$$

From equations 2.7, 2.8, 2.9 and 2.10,

$$KP_0\tau_d = \varepsilon_R - \varepsilon_U = f(0) \qquad (2.11)$$

Hence,

$$\varepsilon^*(\omega) = \varepsilon_U + \frac{\varepsilon_R - \varepsilon_U}{j\omega\tau_d + 1} \qquad (2.12)$$

Separating out the real and the imaginary parts, expressions for relative permittivity and the loss factor are obtained.

$$\varepsilon' = \varepsilon_U + \frac{\varepsilon_R - \varepsilon_U}{1 + (\omega\tau_d)^2} \qquad (2.13)$$

$$\varepsilon'' = \frac{(\varepsilon_R - \varepsilon_U)\omega\tau_d}{1 + (\omega\tau_d)^2} \qquad (2.14)$$

These equations were first developed by Debye (1929). The frequency dependence of ε' and ε'' expressed by equations 2.13 and 2.14 is illustrated in figure 2.5.

In the presence of ionic impurities, the loss factor has one more term which accounts for the conductivity(σ). The resulting expression is,

$$\varepsilon'' = \frac{\sigma}{\omega\varepsilon_0} + \frac{(\varepsilon_R - \varepsilon_U)\omega\tau_d}{1+(\omega\tau_d)^2} \qquad (2.15)$$

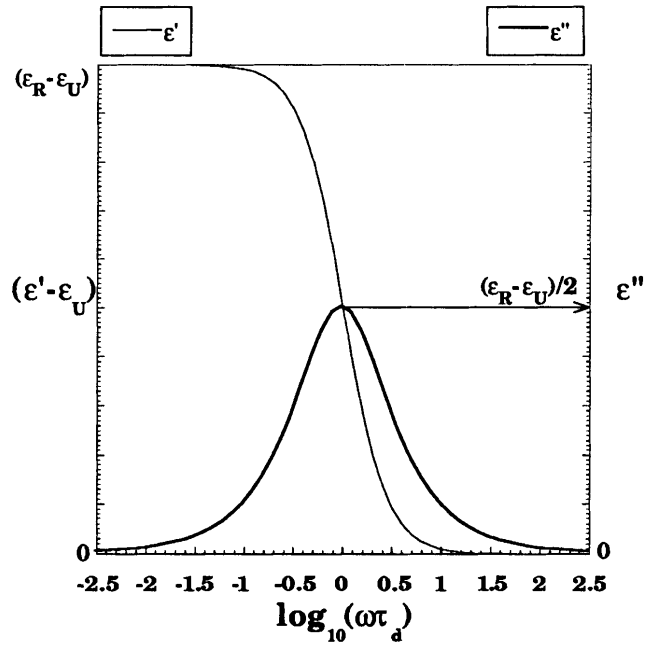

Figure 2.5 : Dependence on frequency of ε' and ε" as expressed by Debye's equations.

2.1-3 Electrode Polarization

The applied electric field polarizes the electrodes and attracts the ions of opposite charge. These ions accumulate at the electrodes and reduce the effective inter-electrode distance as shown in figure 2.2. This effect is significant at the lower frequencies. Thus, at

lower frequencies for a given voltage, the effective field is much greater than that calculated. Hence, the dipoles are much more oriented than they would have been without the electrode polarization (figure 2.1). Therefore, as the frequency of the applied voltage is lowered, the permittivity does not level off to ε_R, but keeps on increasing.

The method to account for electrode polarization has been described earlier [Sheppard, 1986]. From equation 2.5, it can be inferred that the dielectric is modelled as a parallel R-C circuit element. The electrode polarization is dominant in the region where ε'' is greater than ε'. Since electrode polarization causes the measured dielectric properties to be erroneous, it is necessary to only consider data in that region of the frequency sweep where ε'' is less than ε'. In most cases, one can obtain the unrelaxed permittivity, ε_U at the highest frequencies. The methods to obtain the relaxed permittivity are explained in section 4.2.

2.2 Polyimide Chemistry

Polyimides are cyclic chain polymers and are identified by the imide functional group which is made up of a cyclic secondary amine bound to two carbonyl groups with aliphatic or aromatic groups in the main chain. The synthesis of this material is a two stage process. The first is a polycondensation reaction between an acid anhydride and a difunctional base. The product of this reaction is a polyamic acid, which is soluble in highly polar organic solvents such as NMP. In the second stage, thermal imidization (i.e. cyclodehydration reaction with loss of water and the closure of the imide ring) is carried out. This process is illustrated in figure 2.6. This investigation will focus on the second stage of the synthesis process, as it is carried out in the integrated circuit fabrication industry.

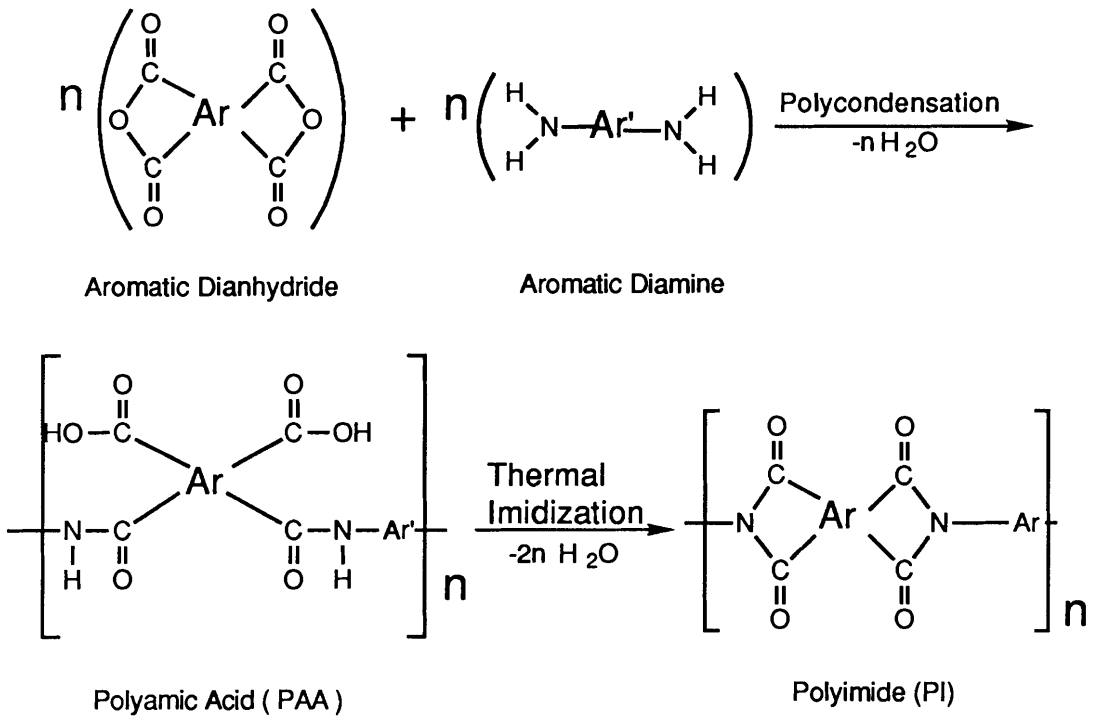

Figure 2.6: Synthesis of polyamic acid and its imidization to polyimide

2.3 Monitoring Degree of Imidization

2.3-1 A Review of Different Methods to Monitor Extent of Imidization

(a) Dynamic Mechanical Thermal Analysis / Thermal Mechanical Analysis (DMTA / TMA):

This method involves monitoring the Young's modulus and loss tangent during the imidization. In the experiments performed on the imidization of PMDA-

ODA (pyromellitic dianhydride - oxydianiline) polyamic acid [Feger, 1989], polyamic acid films were prebaked on glass plates, peeled off and imidized on a DMTA at various heating rates. The results have essentially been qualitative, with the softening temperature being a measure of the extent of imidization [Simoff et al., 1990]. Also, this method requires free-standing films. Polyimide films used in microelectronics are on a substrate. It is very difficult to remove the film from the substrate. There is also the danger of changing the properties (i.e. orientation) of the film as it is peeled off from the substrate. Hence, this method has the drawbacks of being only qualitative and having low potential for providing accurate, in-situ, structural information.

(b) Thermogravimetric Analysis (TGA):

This method involves the monitoring of weight loss during imidization. This weight loss has been attributed to the loss of the decomplexed solvent, NMP and the loss of the water of imidization [Simoff et al., 1990], [Brekner and Feger, 1987]. This loss of weight has then been correlated to the extent of imidization [Simoff et al., 1990]. In this method also, it is necessary to peel off the prebaked film from the silicon wafer and put it in the pan in the TGA. Therefore, this method is not an in-situ method. In addition, this procedure could change the properties of the film.

(c) Differential Scanning Calorimetry (DSC):

DSC has been used to monitor extent of imidization [Navarre, 1982]. In this method, the samples were imidized in pans, each for different times, from zero to 100 minutes, at a particular temperature. This was repeated at different temperatures from 135°C to 320°C. The DSC scan was performed on each sample. The

endothermic peaks were observed between the temperatures 200°C and 300°C. These peak areas decreased with reaction time, and were measures of the degree of imidization.

The problems with using DSC to monitor the imidization reaction are that the samples are not thin films on suitable substrates and that the scans are destructive. Also, this method is not very sensitive to the fine changes taking place towards the end of the reaction.

(d) Fluorescence Spectroscopy:

This method is currently under study by Wachsman and Frank (1988). This technique involves the absorption of radiation in the 320-590 nm, followed by the fluorescence in a higher wavelength region of the spectrum. The sample is a polyimide spin coated on a quartz wafer and thermally imidized. Samples were reacted at different temperatures. The two absorption peaks at 352nm and 486nm as well as the fluorescence peaks and their shifts between 562nm and 592nm were observed as a function of the imidization temperature. The intensities of the peaks increased significantly with reaction temperature from 200°C to 450°C. This shows the high sensitivity of the technique even at high conversions. This method has been postulated to indicate the molecular arrangement as well as the composition.

(e) Mass Spectrometry:

This technique determines the amount of solvent and water outgassed after a particular stage in the imidization process has been reached. One disadvantage with this technique is that it cannot be determined whether the evolved volatiles are due to decomplexation or whether they are the products of a chemical reaction. Hence this technique gives only a qualitative measure of the extent of reaction. Also, since

this method involves destructive testing at each stage of the imidization, it cannot be used for on line monitoring.

(f) Electrical Conduction:

Another method is the measurement of electrical conduction [Ito et al., 1990] as a function of the extent of imidization. This method can be useful for determining the cure extent of polyamic acid formed by vapor deposition polymerization. The drop in electrical conduction has been correlated to the extent of imidization by the increase in the activation energy for the conduction by ion hopping transport. This method involves the vapor deposition of PMDA-ODA polyamic acid along with stoichiometric quantities of unreacted PMDA and ODA on a gold plated surface. Different samples are treated to high temperatures in an oven for different time periods. Subsequently, the polymer has gold evaporated on top of the film. The surface area of the gold plating is about $4mm^2$. However, the disadvantage in using this method is that it is not in-situ.

(g) Solvent Resistance:

This method involves determining the effect of various solvents on the material during the various stages of the imidization. It makes use of the increase in solvent resistance of the material during the imidization process. Hence, this technique is a qualitative measure of the extent of imidization. It cannot be used for on-line monitoring as it is destructive in nature. The solvent effects are listed in table 2.1.

Table 2.1 Dissolution behavior of DuPont PI-2566 after 30 min immersion in solvent [Soane and Martynenko, 1989].

Solvent	Bake Temperature	Effect
NMP	120°C	Dissolved
NMP	135°C	Swelled
NMP	200°C	Crazed
NMP	300°C	No effect
Acetone	120°C	Swelled
Acetone	200°C	No effect

(h) Fourier Transform Infra Red Spectroscopy (FT-IR) :

This method involves the use of the effect of concentration of a species on the absorption of radiation at particular frequencies. FT-IR spectroscopy is used for on-line monitoring and is discussed in detail in section 2.3-2. It has the advantage of providing the structural information directly. One disadvantage of this method is the effect of the absorption of bands neighboring the bands of interest. It is difficult to separate out these effects. Also determining the baseline is largely a trial and error process.

2.3-2. FT-IR Spectroscopic Analysis of Imidization of Polyamic Acid

In order to use this method to follow the imidization reaction, it is necessary to identify the IR bands that are absorbed by either the reactant or the product. It is

conventional and perhaps more accurate to monitor the product formation rather than the disappearance of the reactant. The major bands that have been established as those due to imide absorption are [Pryde, 1989-a] :

- 1780 cm^{-1} : Symmetric stretches of carbonyl groups coupled through five member ring.
- 1720 cm^{-1} : Asymmetric stretches of carbonyl groups coupled through five member ring.
- 1370 cm^{-1} : C-N stretch of imide ring.
- 720 cm^{-1} : Deformation of imide ring or imide carbonyl groups.

For a reactive system, it is necessary to have an internal reference, which will account for the change in the environment of the absorbing groups. In the present case, the ratio of the sum of the number of amic acid groups and the imide groups to the aromatic groups is constant. Hence, it is advisable to correlate the degree of imidization to the ratio of an imide absorption band to that of an identified aromatic absorption band.

- 1015 cm^{-1} : Aromatic vibration peak [Snyder and Painter, 1989].
- 1500 cm^{-1} : Breathing or ring-stretching mode of aromatic moieties [Pryde, 1989-a]

The 1780 cm^{-1} band ratioed with the 1015 cm^{-1} band has been correlated [Snyder and Painter, 1989] to extent of imidization. However, the formation of anhydride and isoimide (1850 cm^{-1} and 1795-1820 cm^{-1} respectively) interfere with the 1780 cm^{-1} band and the isoimide [Pryde, 1990] and the isoimide band (920-935 cm^{-1}) interferes with the 1015 cm^{-1} band. Hence, the ratio of the absorbances of the 1370 cm^{-1} band to the 1500 cm^{-1} band has been accepted as the measure of the degree of imidization [Pryde, 1989-a]. This band needs to be normalized to the ratio at full conversion. Hence, an external

standard of the complete imidization ratio of the absorptions at these bands has been used [Pryde, 1989-a]. Thus, the degree of imidization is given by:

$$x = \frac{\left(A_{1370}/A_{1500}\right)}{\left(A_{1370}/A_{1500}\right)_{\text{FULL IMIDIZATION}}} \qquad (2.16)$$

In equation 2.16, it is important to note that the ratio at full imidization is taken at the temperature of complete imidization. This is an assumption based on earlier work in this area [Pryde, 1989-a], where it was found that during imidization by a ramped temperature schedule, the best results were obtained using the expression:

$$x = \frac{\left(A_{1370}/A_{1500}\right)_{T}}{\left(A_{1370}/A_{1500}\right)_{T_{max}}}$$

It is accepted that temperature affects the absorption spectra [Snyder et al., 1988]. However, these effects change the absorbance by about 1% over a temperature difference from 175°C to 350°C and are hence relatively insignificant. The theory behind temperature effects has been presented by Snyder et al. (1988). The temperature correction at any wave number ν (cm^{-1}), is given by:

$$\frac{A^{\nu}_{T_2}}{A^{\nu}_{T_1}} = \frac{\exp\left(-hc\nu/kT_1\right)+1}{\exp\left(-hc\nu/kT_2\right)+1} \qquad (2.17)$$

In this equation, $A^{\nu}_{T_i}$ is the absorbance at frequency ν in cm^{-1} and temperature T_i°K, c is the velocity of light in cm/sec (3 x 10^{10} cm/s), h is Planck's constant (6.626 x 10^{-34} J-s) and k is the Boltzmann's constant (1.38x10^{-23}J/°K).

2.4 Modelling Dielectric Property Changes with Chemical Structure

2.4-1 Dielectrometric Analyses of Thermosetting Resins

Of the many advances in the dielectric analysis of polymers, most have been only in the realm of thermosetting polymers. Kienle and Race (1934) were the pioneers in this area when they first tried to correlate the extent of reaction of a polymer to its dielectric properties. Successive studies have emphasized the crosslinking reactions of oligomers. The materials of interest have been resins (i.e. various epoxies, polyesters, phenolics, polyimides, rubber, shellac and other resins) as well as composites (i.e. epoxy with glass, graphite or other fillers, and polyimide with graphite) [Senturia and Sheppard, 1986]. Recent advances in this field have allowed cure monitoring of urethane and in applications with extremely fast reactions (i.e. reaction injection molding) {[Holmes and Trask, 1988], [Sheppard et al., 1989]}. Dielectric analysis has also been performed for the cure of thermosetting polyimides [Kranbuehl et al., 1982]. The common denominator has been that the starting reactant has always been a polymer or an oligomer. The nature of the polymerization being monitored has been a cross-linking process.

Efforts have been made to correlate the extent of the cure process to the dielectric properties. In the case of epoxies, the dielectric properties have been correlated to the

viscosity change during cure. The empirical Williams-Landell-Ferry derivation from the free volume model has been used to model the relationship between conductivity and extent of cure {[Sheppard, 1986], [Bidstrup, S. A. et al., 1989]}. A more fundamental free volume ionic conductivity model has been developed [Simpson, 1989] based on another free-volume viscosity model [Berry and Fox, 1968]. The basis of the free volume ionic conductivity models is that ionic mobility is correlated to the amount of free volume in the system which changes with the degree of reaction.

2.4-2 Dielectrometric Analyses of Thermoplastic Polyimides

Thermoplastic polyimides are formed by imidization (i.e. curing) of polyamic acid. Though this reaction is not a crosslinking reaction, the change in chemistry during the reaction causes significant changes in the dielectric properties. Therefore, there is potential for monitoring this reaction also by dielectrometric method.

Dielectrometric analysis of imidization was performed at low temperatures (i.e., incomplete imidization) [Day and Senturia, 1982]. Although they reported both parts of the dielectric constant, these researchers too suggested the use of loss factor to determine the extent of reaction and the method of using the change in ionic conductivity as a measure of the extent of reaction.

The trend in dielectrometry so far, has been in the use of the loss factor, and thus, the ionic conductivity as a measure of the degree of cure. In the present investigation, change in permittivity is proposed as a measure of the degree of imidization. This is because, permittivity is related to the dipole moment, which depends on the chemistry. The reaction causes a change in chemistry resulting in change in dipole moment in the system, which can be correlated to changes the permittivity. Modelling cures using ionic

conductivity and loss factor have entailed the determination of Tg of the material at every stage of the reaction {[Sheppard, 1986], [Bidstrup, S.A. et al., 1989]}. It is very difficult to determine the Tg of thermally imidizing polyamic acids or partially imidized polyamic acid (eg. PMDA-ODA polyamic acid), because imidization might occur during the temperature scan needed to be performed to determine Tg. Hence it would be very difficult to model the imidization of polyamic acid using the loss factor.

To relate permittivity to the extent of reaction, it is necessary to determine the relationship of permittivity to structural features. Debye [1929] determined the relationship between dipole moment and the dielectric constant. This was improved upon by considering the effects of the field produced due to externally acting field and the field produced by the dipole [Onsager, 1936]. Then the effect on the dielectric constant due to two interacting dipoles was also determined [Frölich, 1958]. These developments have been made applicable to homopolymers having only one type of dipole unit [McCrum et al., 1967]. The effect of molecular structure on dipole moment was developed earlier [Smyth, 1930]. Thus, the basis for determining the dielectric constant from molecular structure and vice versa is available. Hence, the present investigation uses this to extend the structure-property relationships to reactive polymer systems (eg. imidizing polyamic acid) where different types of dipoles (amic acid and imide dipoles) are distributed within the system.

CHAPTER III

EXPERIMENTAL METHODS AND RESULTS

3.1 Chemical System

This investigation is concerned with the imidization of a polyamic acid, which, as described in section 2.2, is formed by a polycondensation reaction between an acid anhydride and a difunctional base. The polyamic acid used was Du Pont PI-2542 which consists of pyromellitic dianhydride (PMDA) as the acid anhydride, and oxydianiline (ODA) as the difunctional base. It was obtained as a solution in a highly polar solvent, n-methyl pyrrolidinone (NMP). It was stored at temperatures below 4°C to prevent any imidization from taking place during storage. The solution was allowed to come to room temperature before use so as to prevent any moisture from condensing onto the solution. In solution form, the polyamic acid has four NMP molecules attached to each amic acid unit [Brekner and Feger, 1987].

This material first undergoes a pre-bake step which involves heating the material to approximately 100°C to evaporate out the unbound solvent. The residue is polyamic acid complexed with NMP in the ratio of 4 NMP molecules per amic acid repeat unit. Continuation of the pre-bake step causes further decomplexation to give a residue of

polyamic acid complexed with NMP in the ratio of 2 NMP molecules per amic acid repeat unit [Brekner and Feger, 1987]. The pre-bake step is shown in figure 3.1

The pre-bake step is followed by the actual baking step. This involves heating the material up to 300°C or 400°C. During this step ring closure or imidization occurs. For every amic acid unit that imidizes two water molecules and two NMP molecules are evolved.

3.2 Measurement of Dielectric Properties during Imidization

3.2-1 Experimental Procedure

A Micromet Instruments Eumetric System III Microdielectrometer was used to determine the dielectric properties as function of reaction time throughout the imidization. The Micromet system uses a silicon integrated circuit sensor which consists of a comb electrode pattern, a system of field effect transistors (FETs) to amplify the signals and a semiconductor thermal diode for temperature measurement. Figure 3.2a shows a schematic of the microdielectrometer configuration. A more detailed diagram of the sensor is illustrated in figure 3.2b [Micromet Instruments, 1985].

An organosilane adhesion promoter is required to ensure good adhesion between the polymer and the sensor surface. This was prepared by mixing 95ml of methanol, 5ml of deionized water and adding 0.05ml of Pyralin VM-651 adhesion promoter supplied by Du Pont. The final mixture was sealed and refrigerated for at least 12 hours before use. The shelf life of this solution was three weeks.

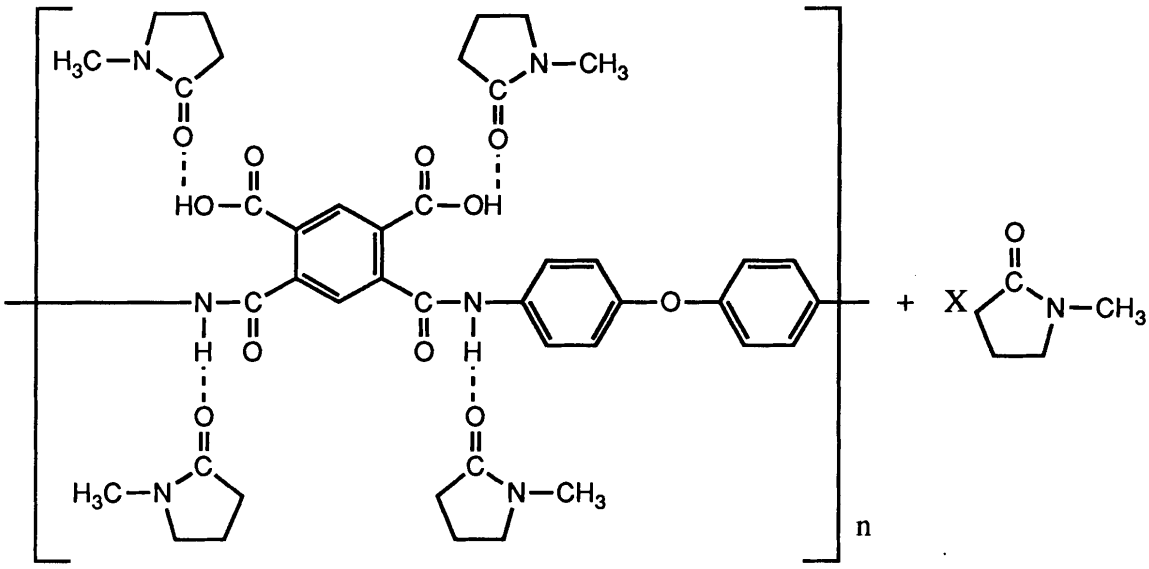

Solute - Polyamic Acid (PAA) - each Amic Acid unit complexed with 4 NMP molecules

Unbound Solvent - NMP

1 Hr Prebake @100°C

-(2n+X)NMP

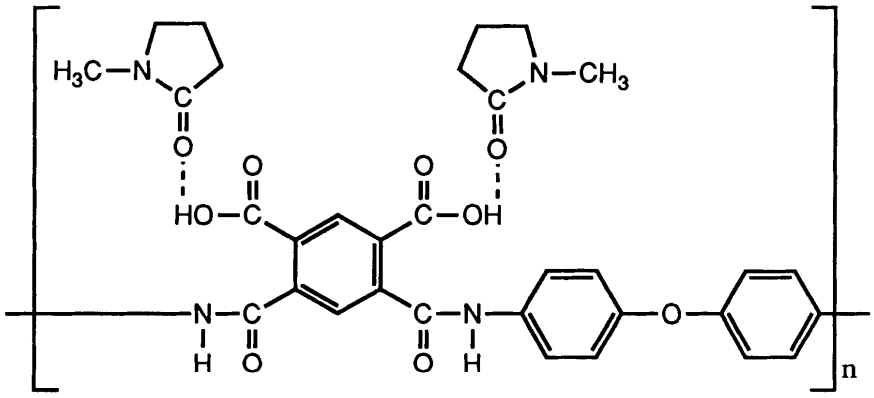

Polyamic Acid (PAA) - each Amic Acid unit complexed with 2 NMP molecules

Thermal Imidization

-2 (NMP + H_2O)

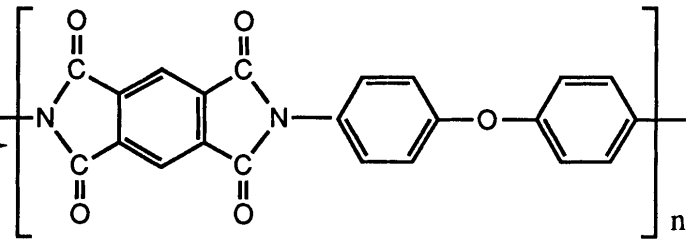

PMDA-ODA Polyimide (PI)

Figure 3.1: The prebake and the imidization of polyamic acid to polyimide

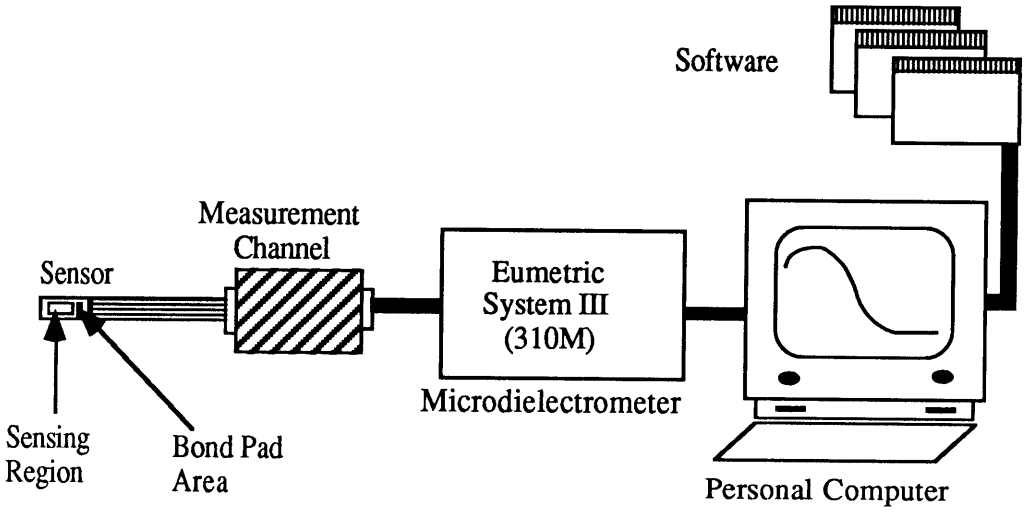

Figure 3.2-a: Basic System III configuration with computer control.

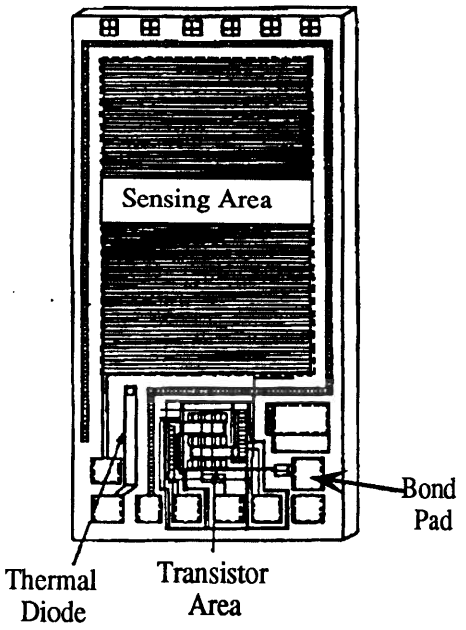

Figure 3.2-b: Detailed sketch of a dielectric microsensor

A clean sensor was tested in air prior to each experiment. The sensor was considered acceptable if the measured gain in air was between -39 and -43 db and the measured phase was between -2 and 2 degrees when voltage was applied at frequencies in the range from 1 Hz to 10 kHz [Micromet Instruments, 1985]. If the sensor failed this air test, it was cleaned with acetone, oven dried and tested again. The sensor was then dipped in an adhesion promoter solution and dried in air. The sensor was tested again until the gain and phase measurement were found to be in the acceptable regime for air. This indicated that the methanol and the water had evaporated. The sensor was subsequently dipped in the polymer solution so that the entire sensing surface of the sensor was covered with the polymer. Extreme care was exercised to prevent any of the sample from flowing onto the bond-pad area on the sensor. This precaution was necessary because shrinkage of the polymer surface during the reaction results in stresses that can break the connection at the bond pads.

The sensor with the sample was then placed on a circular NaCl window using a double-sided tape. The window was 32 mm in diameter and 3 mm thick. The sensor was connected to the dielectrometer and the salt window was placed on top of a Fisher Thermix® stirring hot plate. The sample was pre-baked by heating on the hot plate for one hour at 100°C to remove the unbound solvent. The reason for pre-baking the sample on the hot plate was to first rigidify the layers in contact with the sensor sensor. Thus, it would be possible for the evolved volatiles to diffuse or bubble out through the more fluid upper layers. In this way the possibility of any bubbles remaining entrapped in the sample was greatly reduced. The pre-bake was carefully monitored to manually remove any bubbles that might still have remained otherwise. The sample on the sensor was cooled to room temperature. This was done to enhance the uniformity of temperature schedules for the subsequent thermal treatment for imidization.

The salt window with the sensor were then put into the Spectra Tech Heated Demountable Cell, HT-32. A schematic of the cell is shown in figure 3.3. The temperature of the cell was controlled by a Spectra Tech Microprocessor Programmable Temperature Controller. Isothermal imidization reactions were carried out at 130°C, 160°C and 200°C. The same heating schedule was used for all the reactions at a particular temperature. This was facilitated by the cooling of the sample to room temperature before imidization. Thus, the heating rate to an imidization temperature could be kept uniform for all samples. Dielectric measurements were made by carrying out frequency sweeps every five or ten minutes from 100 Hz to 100 kHz in thirty steps. It took approximately four minutes to perform each frequency sweep.

3.2-2 Experimental Results

The permittivity (ε') as a function of time during the pre-bake is shown in figure 3.4-a. At higher frequencies, only the most mobile dipoles align with the applied electric field during the cycle time. Therefore, the permittivity decreases as frequency of the applied voltage increases. At low frequencies, more dipoles orient and the ionic impurities have more time to move towards their respective electrodes. Hence, the ions accumulate at the electrodes and decrease the effective distance between them. Therefore, for the same potential difference between the electrode plates, the electric field would be much higher due to the electrode polarization caused by ion accumulation. At still lower frequencies, the effect of electrode polarization increases. Hence, the measured value of the permittivity would be greater than the actual value.

During the first twenty minutes of the pre-bake, the permittivity remained approximately constant. In the first forty minutes, the temperature of the sample was raised

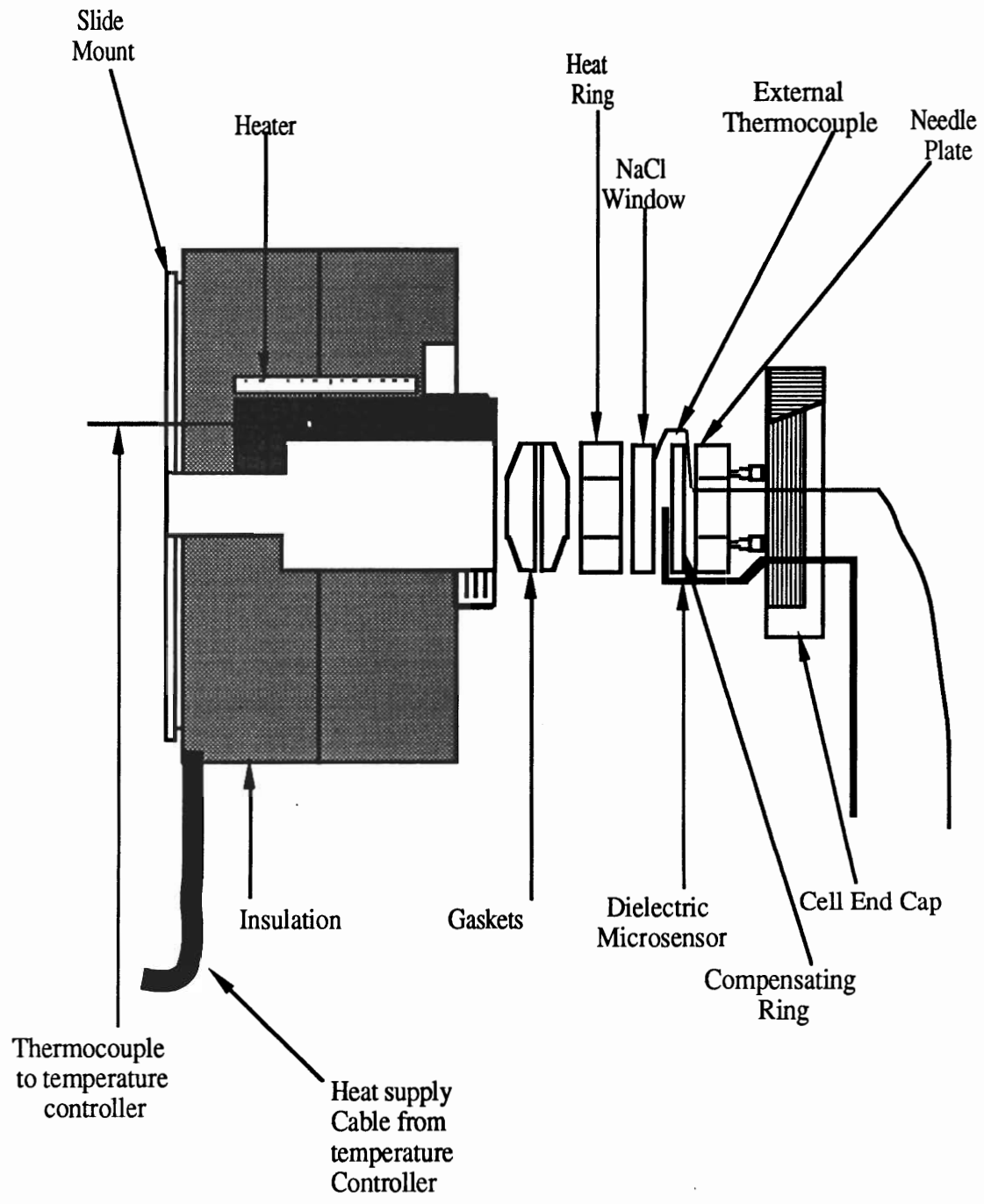

Figure 3.3: Schematic of the heated demountable cell showing the position of the dielectric microsensor .

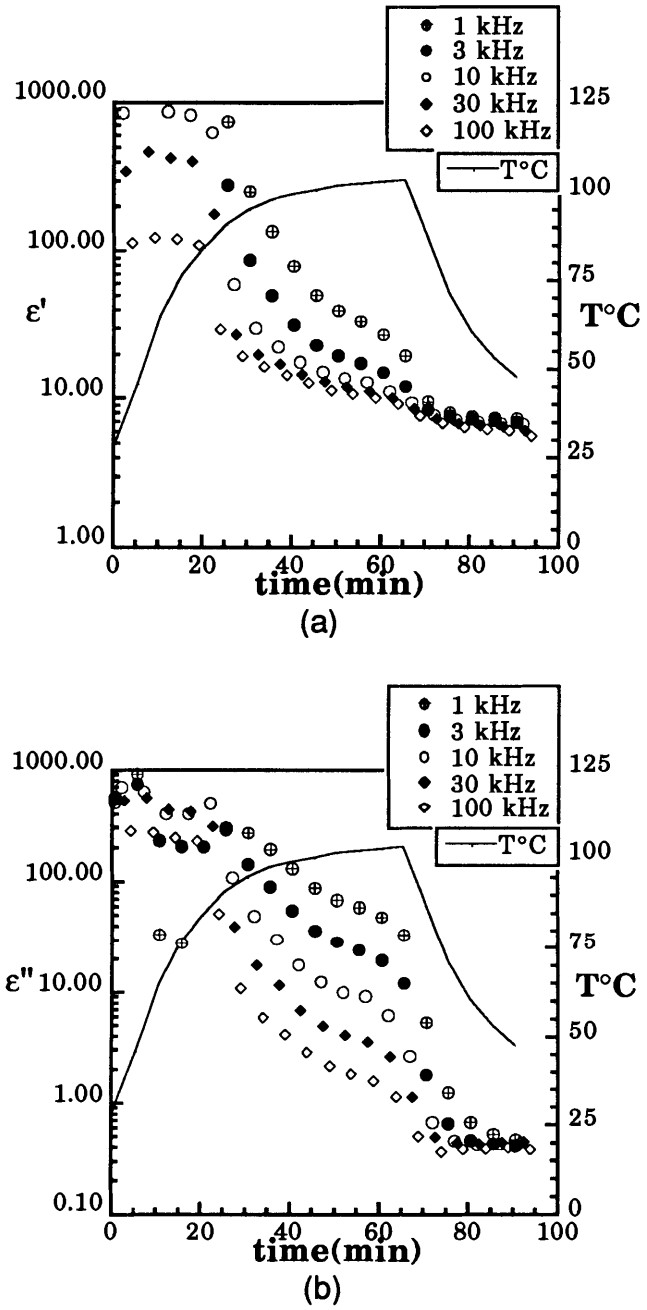

Figure 3.4: Dielectric response during the pre-bake:
(a) permittivity (b) loss-factor.

from room temperature to the pre-bake temperature of 100°C. Hence, a possible explanation for the constant permittivity observation in the first twenty minutes is that, raising the temperature gives rise to some factors that cause the permittivity to increase and their effects are cancelled by some other factors that cause the permittivity to fall.

The possible factors that might cause the permittivity to rise during the period in which the temperature is raised are the increase in molecular mobility and decrease in solvent viscosity. Increase in molecular mobility due to increase in temperature facilitates the alignment to dipoles along the applied electric field. Lowering the viscosity of the solvent would permit the ionic impurities more freedom to move towards their respective electrodes. This would give rise to their accumulation at the electrodes. Hence, the measured permittivity would appear to be much higher due to electrode polarization.

A factor that could cause the lowering of the permittivity during the rise in temperature could be a the loss of unbound solvent. Besides decreasing the quantity of polar units, a rise in viscosity of the polymer would restrict dipole motion. Solvent loss would also inhibit the movement of the ionic impurities by raising the viscosity. Thus, the effect of electrode polarization i.e. the accumulation of the ionic impurities at the electrodes would decrease.

The subsequent monotonic decrease of the permittivity after 20 minutes of pre-bake could be attributed to loss of unbound solvent. After a pre-bake of one hour, most of the unbound solvent is assumed to be removed. This can be seen in the near leveling off of the high frequency permittivity. Further heating might cause perceptible imidization. Although imidization begins the moment the temperature of the material rises above 4°C, it is not easily discernible at this stage of the processing. This will be demonstrated through the FT-IR studies which will be described later.

After the hot plate is switched off and the temperature has dropped, it is noted that the permittivity also drops due to an increase in viscosity of the polymer. The difference between the high frequency permittivity and the low frequency permittivity also drops significantly with temperature. As seen in equation 2.11, the frequency dependent part, which corresponds to the orientation of all dipoles, is a multiple of $(\varepsilon_R-\varepsilon_U)$. Hence, the frequency dependent part of the permittivity can be seen to decrease with decrease in temperature. This is because dipole mobility decreases with decrease in temperature. Also, the degree of electrode polarization decreases, thus reducing the effect of the lowering of the frequency.

In figure 3.4-b the plot of loss factor during the pre-bake is shown. The behavior of loss factor in the first 20-25 minutes will not be analyzed due to the dominance of electrode polarization in this region. After 25 minutes, the rate of temperature increase has dropped sharply. At this point, the number of NMP molecules attached to the each amic acid starts decreasing from four to two. This would increase the packing of the polymer molecule, thus lowering the mobility of the ionic species, causing the conductivity to drop. Further lowering of the loss factor after the switching off of the hot plate could be possibly attributed to the lowering ionic mobility caused by the reduction of temperature only. Thus, the conductivity reduces even after the pre-bake has ended. A drop in temperature also results in lowering of the amplitude of the oscillation of the dipoles due to the lowering of the free volume.

It is observed that electrode polarization affects the data during the early stages of the imidization. The frequency response of polyamic acid after 20 minutes of imidization at 130°C is shown in figures 3.5-a and 3.5-b. It is observed that both, the permittivity and the loss factor rise with decrease in frequency of the applied voltage. The increase in permittivity with decrease in frequency is monotonic. It does not level off to a limiting

value, ε_R. In figure 3.5-b, it is observed that ε'' versus frequency is almost a straight line with a slope of -1 on a log-log scale. On considering equation 2.15, the first term containing the conductivity is seen to be the dominant contribution to the loss factor.

The dielectric response of the sample during imidization at 130°C, 160°C and 200°C is illustrated in figures 3.6, 3.7 and 3.8 respectively. At lower frequencies, the dipoles orient to a greater extent and resulting in higher permittivities than at higher frequencies. Also, the ionic conductivity term in the loss factor decreases with increasing frequency and causes the loss factor to decrease.

Observing the response of change in permittivity during imidization (figures 3.6-a, 3.7-a and 3.8-a), it is noted that the permittivity drops rapidly initially and then levels off. The explanation for this behavior is that, during imidization, the more polar reactant amic acid units complexed with NMP molecules are converted to imide units which are much less polar. In addition, the polymer molecules become more closely packed during imidization. This reduces the mobility of the dipoles, thus reducing the permittivity.

The final value of the permittivity, at the end of the imidization at a particular temperature, also has significance. Earlier studies {[Laius et al., 1967], [Laius and Tsapovetsky, 1982], [Osredkar, 1988], [Pryde, 1990]} have shown that the extent of imidization is greater at higher imidization temperatures. The permittivity after three hours of imidization at 130°C is about 5, that after two hours at 160°C is about 3.8 and that after one hour at 200°C is about 3.3.

As observed in figures 3.6-b, 3.7-b, 3.8-b, during the imidization at each of the three temperatures, the loss factor also showed an initial rapid decrease followed by a leveling off. This decrease can be related to the fact that there is a conversion from a more polar material to a less polar material. Hence, as described in section 4.1 the polar groups change from the bulky amic acid group to the much smaller diphenyl ether group. Thus the

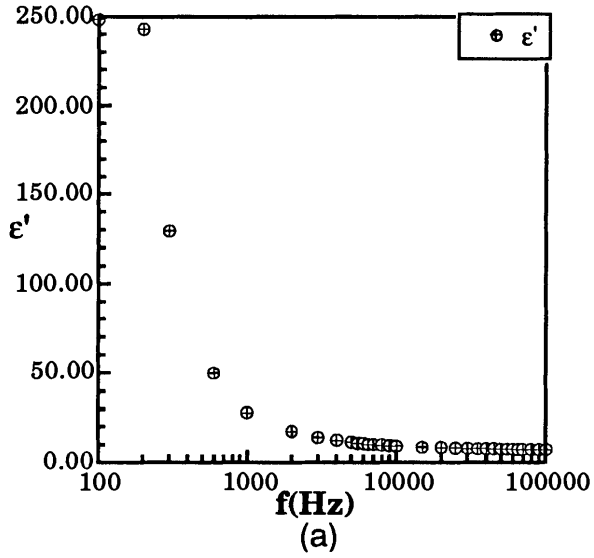

(a)

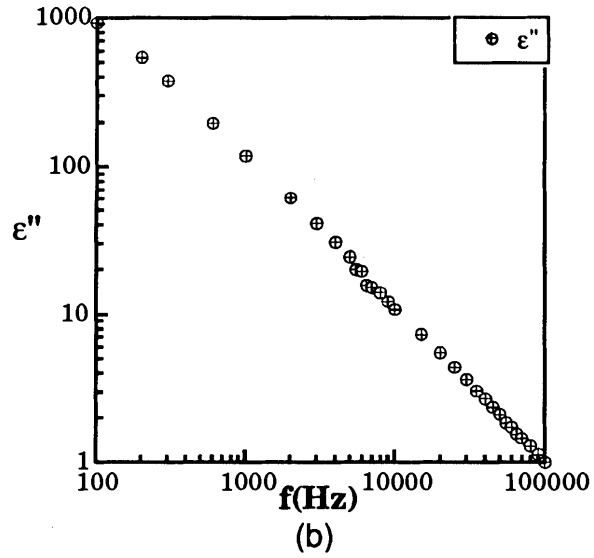

(b)

Figure 3.5: Frequency response of dielectric properties of polyamic acid after 20 minutes of imidization at 130°C : (a) permittivity (b) loss factor.

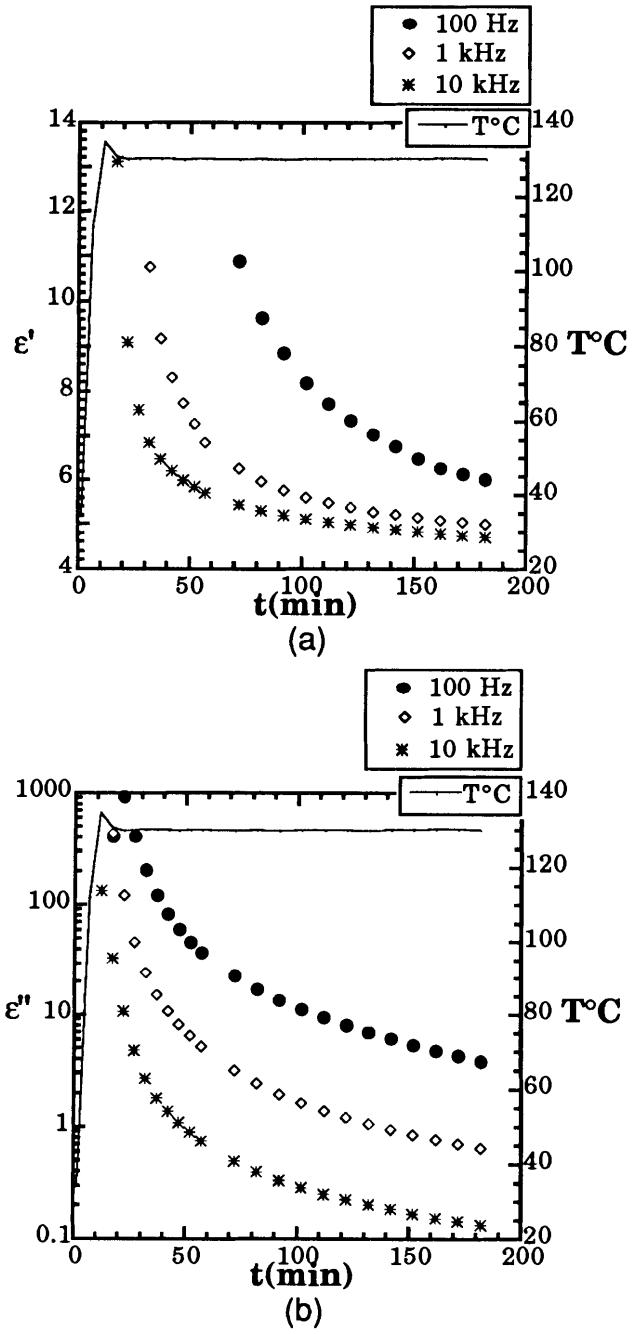

Figure 3.6: Dielectric monitoring of the imdization of polyamic acid at 130°C: (a) permittivity (b) loss factor.

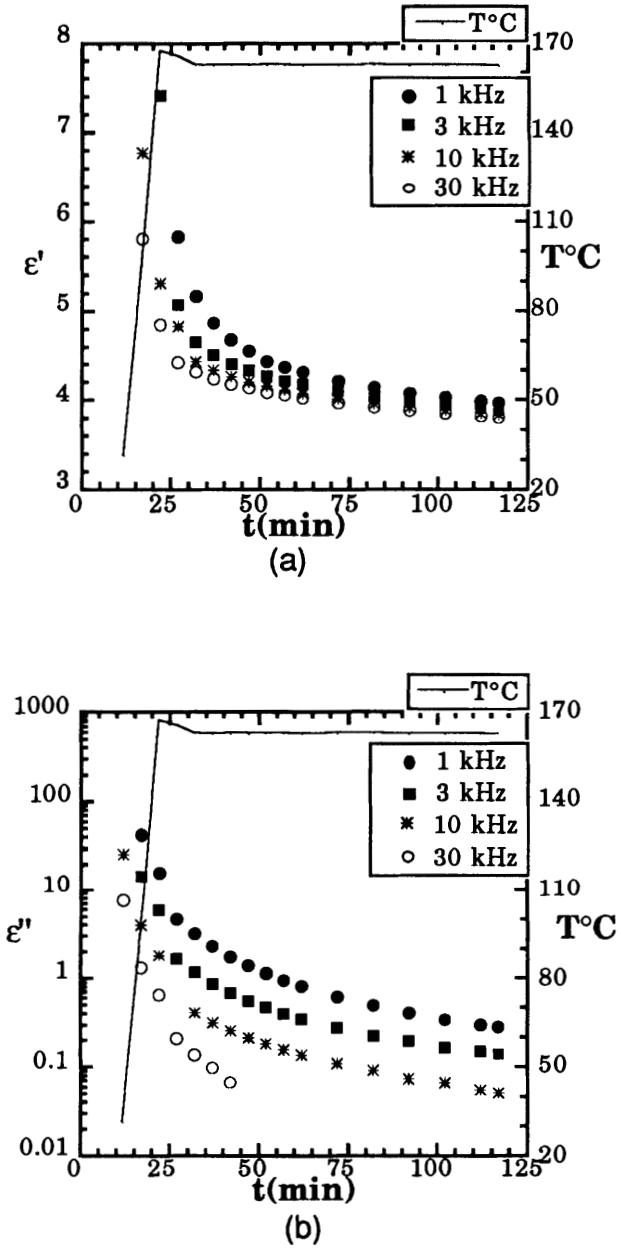

Figure 3.7: Dielectric monitoring of the imdization of polyamic acid at 160°C: (a) permittivity (b) loss factor.

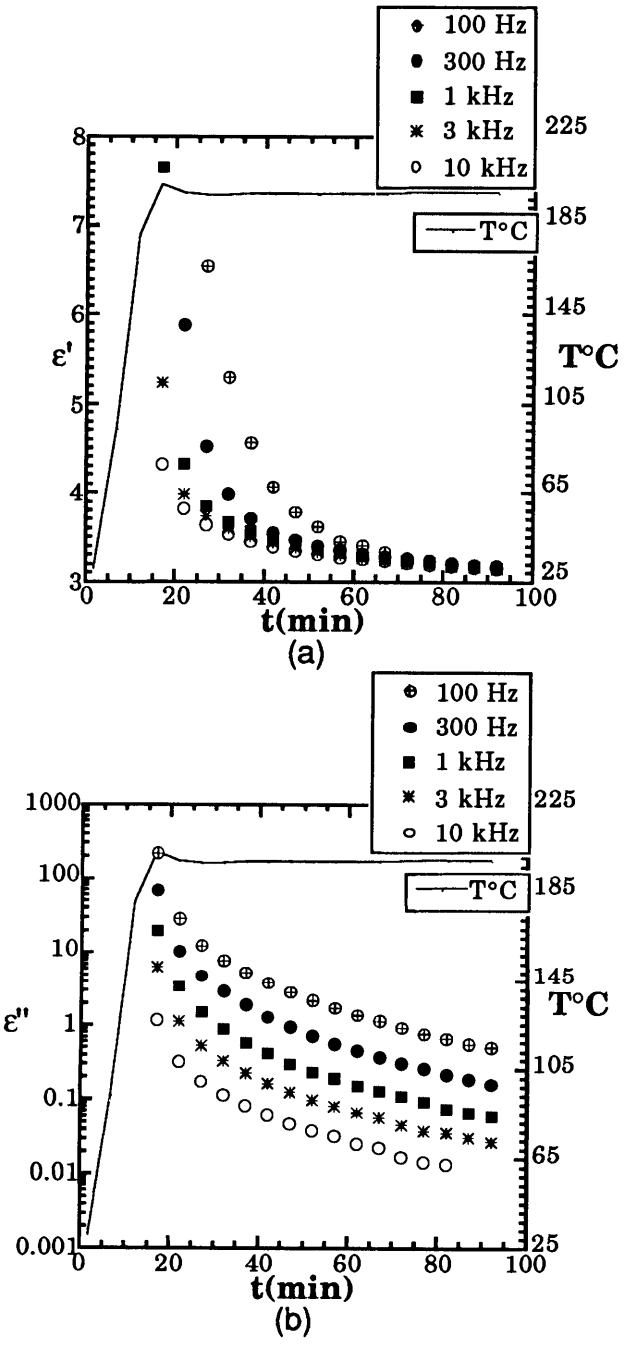

Figure 3.8: Dielectric monitoring of the imdization of polyamic acid at 200°C: (a) permittivity (b) loss factor.

energy losses in the orientation of the the imide group are very small. Also, the close packing resulting due to imidization drastically reduces the mobility of the ions, thus reducing the conductivity and resulting in low values for ε".

3.3 Measurement of Extent of Imidization

The sample storage method and the pre-use thawing were the same as described in section 3.1-1. The polymer solution was spin coated on a clean, polished NaCl window at 7000 rpm and was pre-baked on the hot plate at 100°C along with another salt window holding the dielectric microsensor. This was done so that the samples for both dielectric analysis and FT-IR spectroscopic analysis have identical pre-bake thermal histories. The typical heating schedule for the pre-bake can be seen in figure 3.4.

The thermal imidization was carried out by heating the window in a Spectra Tech Heated Demountable Cell [HT-32], controlled by a Spectra Tech Microprocessor Programmable Controller. The temperature schedule used for the FT-IR spectroscopic measurements was identical to the schedule used for the dielectric measurements. The cell was placed in the sample chamber of a Nicolet 60SX FT-IR Spectrometer. Isothermal reactions were carried out at 130°C, 160°C and 200°C and scans were taken every five minutes. The extent of reaction was determined by the following equation as described in section 2.3-2.

$$x = \frac{\left(A_{1370}/A_{1500}\right)}{\left(A_{1370}/A_{1500}\right)_{\text{FULL IMIDIZATION}}} \qquad (2.16)$$

In this equation, A_{1370} is the absorbance peak height of the 1370 cm^{-1} band which corresponds to the C-N stretch of the imide ring and A_{1500} is the absorbance peak height of the 1500 cm^{-1} band corresponding to the skeletal aromatic ring stretch.

To determine the denominator, the ratio of imide absorbance to aromatic absorbance at complete imidization, it was necessary to determine the point of 100% imidization. An earlier study [Pryde, 1989-a] showed that for the imidization during which the temperature follows a ramped schedule of about 5°C/min, this ratio reached a maximum at 350°C. In the present investigation the reactions were carried out isothermally, following a ramped schedule of about 15°C/min. To determine the full imidization ratio, reactions were carried out by heating separate samples to 315°C, 350°C and 400°C. The highest ratios obtained in these reactions were noted and the highest among them was taken as the ratio of full imidization. In each of the reactions, at 315°C, 350°C and 400°C respectively, the ratio reached a maximum after which it showed a slight decrease with time (Table 3.1). This indicated that as the sample temperature was constant, the imide fraction tended to decrease due to degradation in air. Another possible cause for the decrease in the ratio is that, the Tg of the sample is rising, approaching the sample temperature {[Palmese and Gillham, 1987], [Pryde, 1990]}. During two of the reactions, when the set points corresponded to sample temperatures of 350°C and 400°C respectively, the highest value of the ratio was reached when the sample temperature reached 350°C. The value was 0.624 and it was taken to be the value for complete imidization. This would cause an error in the resulting value of the

extent of conversion, the error would not be very large, because at 350°C, the reaction is almost complete.

Table 3.1: Determination of A_{1370}/A_{1500} ratio for fully imidized polyimide.

Set Point	315°C		350°C		400°C	
	RATIO	T_{sample}	RATIO	T_{sample}	RATIO	T_{sample}
0			0	25		
5				62		52
10	0.1978	167		151		137
15	0.5871	262		249	0.5117	216
20	0.6077	317	0.6124	320	0.6028	298
25	0.6052	316	0.6228	350	0.6238	354
30	0.6033	313	0.6172	352	0.6220	395
35	0.6035	313	0.6088	352	0.6192	402
40			0.6057	352	0.6040	402
45			0.6026	352	0.5919	402
50			0.5999	352	0.5838	402
55			0.5962	352	0.5765	402
60			0.5959	352	0.5744	402
65			0.5933	352		

The extent of imidization as a function of time at the different temperatures is shown in figure 3.9. Initially, in the first five minutes, there was no discernible reaction as the cell was being heated to the desired temperature. Then the reaction proceeded rapidly, before slowing down. It is seen that the extent of reaction was about 28% after three hours at 130°C. An increase in the degree of imidization was observed even after three hours. At

160°C, the reaction had almost slowed down significantly after an proceeding initially at a high rate and the apparent conversion was 73% within two hours. At 200°C, the reaction was 84% complete after one hour. There is a scatter of about 1% in the apparent extent of imidization at 160°C and 200°C.

Earlier studies [Laius and Tsapovetsky, 1982] suggested that the polyamic acid existed in two conformers, one of which was more favorable for imidization. In unimidized polyamic acid, there would be rapid exchange between conformers. Imidization rigidifies the polymer and virtually stops the exchange. This could be the reason for the rapid arrest in the imidization and perhaps Tg could be rising above the imidization temperature when the imidization seems to have slowed down. After significant imidization has been carried out, raising the temperature to 350-400°C might not release all the conformers less favorable to imidization and imidization might not reach completion. This phenomenon would make the apparent degree of imidization to be much higher than the actual value. Hence, separate samples have to be imidized directly to complete conversion without going through the intermediate partial imidization.

Results of earlier IR analyses carried out on the isothermal imidization to form PMDA-ODA polyimide {[Laius et al., 1967], [Laius and Tsapovetsky, 1982]} showed 60% imidization at 160°C after 80 minutes. The results do not compare with those obtained in the present study because the extent of imidization was given by:

$$x = \frac{(A_{1370})}{(A_{1370})_{\text{FULL IMIDIZATION}}} \qquad (3.1)$$

In equation 3.1, the full imidization absorbance is taken to be after treating the polyamic acid sample to a temperature of 300°C for 15 minutes. These investigations determined that the maximum error in determining the extent of imidization due to shrinkage did not exceed 15%. The results of the present investigation lie within the range described by the earlier investigators.

As mentioned in section 2.3-2, the full imidization ratio is taken at the temperature at which imidization is completed. The effect of temperature on the ratio of the absorbances is shown in figure 3.10. Similar trends were observed in an earlier study [Pryde, 1990] for absorbance ratios of fully imidized BTDA-ODA:MPDA (benzophenone tetracarboxylic acid anhydride - oxydianiline: m-phenylenediamine) polyimide. It is observed that the ratio drops significantly as the temperature is lowered. This is true for the ratios both, at the end of the partial isothermal imidization at 160°C and that at complete imidization at the imidization temperature. If equation 2.17 were to be applied to determine the effect of temperature on the absorbance ratio, then the change will be just 0.6% over the temperature range from 160°C to 350°C. To account for the significant decrease in the value of the ratio, due to cooling the polyimide from 350°C to 160°C, a possible explanation offered is that after complete imidization at 350°C, the material is in the rubbery state at 350°C and cooling it to 160°C might vitrify it [Pryde, 1990]. Similarly, after two hours of reaction at 160°C, the glass transition temperature is probably still lower than the sample temperature, that is the material is in the rubbery state. This is because, as observed in figure 3.10, the absorbance ratio decreases noticeably on cooling the polyimide formed by 2 hours of imidization at 160°C.

It should be noted that the extents of imidization illustrated in figure 3.9 are assumed values of the extent of reaction. This assumption is made on the basis of the discussion in the preceding paragraph. Another basis for the assumption is an earlier study

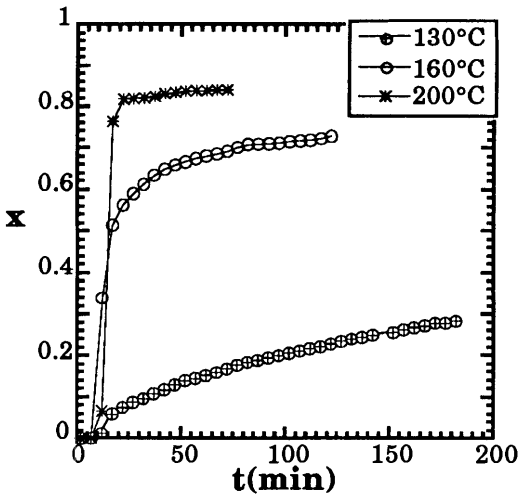

Figure 3.9: Extent of imidization as a function of time as measured using FT-IR spectroscopy.

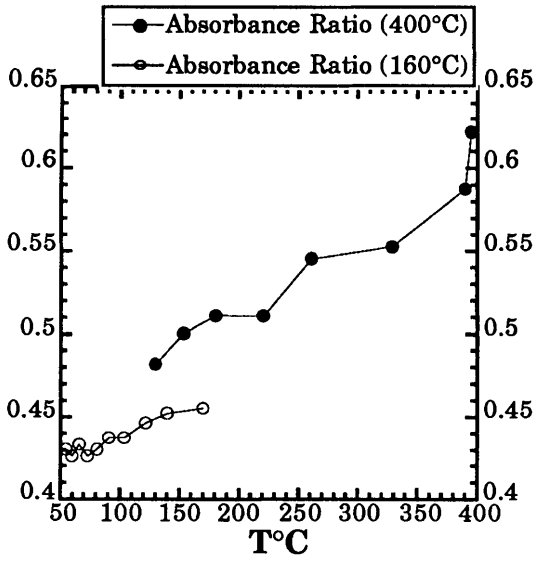

Figure 3.10: Ratio of imide absorbance to aromatic absorbance as a function of temperature for fully imidized and partially imidized polyimide.

[Palmese and Gillham, 1987] which showed that the Tg of polyimide becomes greater than the imidization temperature by only 40°C even after twelve hours of isothermal imidization. It is possible that the Tg of the polymer rises above the imidization temperature within two hours. However, Tg is assumed to be less than the imidization temperature, because such an assumption explains the results observed in figure 3.10, i.e. the absorbance ratio decreases significantly below the imidization temperature. In addition, Pryde (1989-a) obtained reproducible results for the conversion by taking the FT-IR absorbance ratio at the end of the reaction at the imidization temperature. Hence, this method was employed in the present investigation.

3.4 Measurement of Dielectric Properties of Fully Imidized Film.

To measure the dielectric properties of fully imidized polyimide and determining the interaction parameter for fully imidized film, parallel plate capacitor measurements were carried out on Kapton® (PMDA-ODA) film supplied by Du Pont. To ensure satisfactory contact between electrode and dielectric, aluminium electrodes, about 0.5 microns thick, were sputtered on the Kapton® film. Frequency scans were performed at room temperature, 130°C,160°C and 200°C using the parallel plate option of the Micromet System III Microdielectrometer.

The dielectric response of fully imidized polyimide at the different temperatures is shown in figures 3.11-a and 3.11-b. The fall in permittivity due to rise in temperature is counter-intuitive because increase in temperature should increase the mobility of the dipoles, causing them to orient more, giving rise to a higher permittivity. The behavior observed is a decrease in permittivity and the reason for this behavior is not clearly

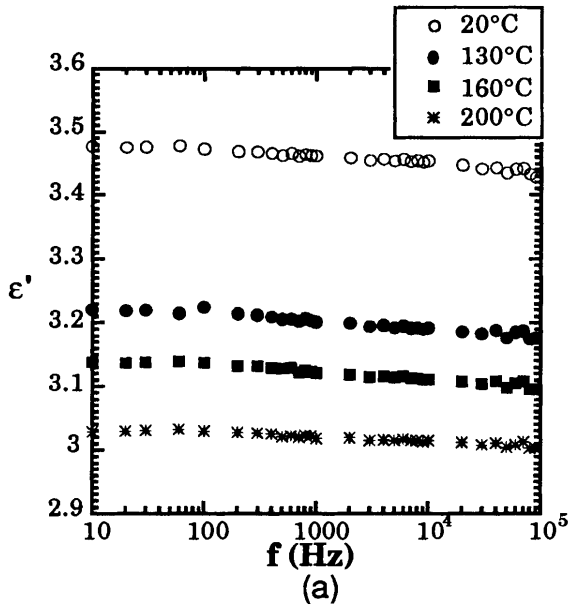

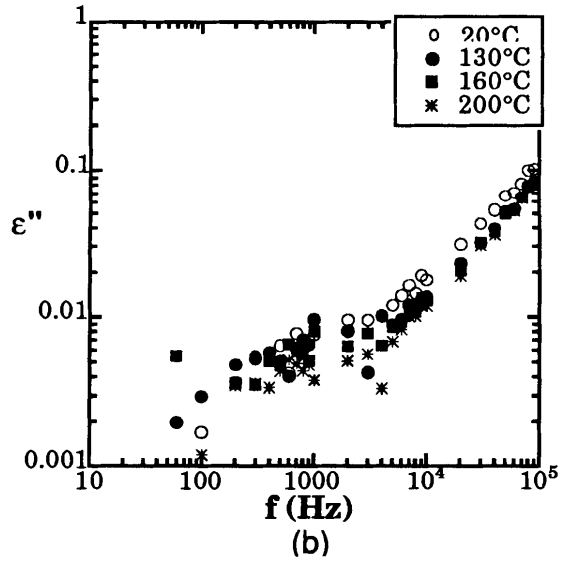

Figure 3.11: Dielectric response of parallel plate measurements on Kapton® film: (a) permittivity (b) loss factor

understood. However, one possible reason is that on heating, moisture is evaporated out of the film by heating. Water is a highly polar substance. Hence, removal of moisture reduces the number of polar units in the system, thus reducing the permittivity.

3.5 Relationship between Dielectric Properties and Extent of Imidization

The imidization of polyamic acid to polyimide has been studied using various characterization techniques. They are summarized in section 2.3 and 2.4. The main purpose of this investigation is to understand the relationship between dielectric properties and molecular structure which would depend on the extent of reaction. An important application of polyimide in microelectronics fabrication processes is as an interlevel dielectric. For this application, the dielectric constant is the critical performance property. Hence it is advantageous to explore this relationship by determining the dielectric properties of the material and the extent of imidization simultaneously. This is the first time that such an investigation has been carried out for polyimides.

The procedure for and results of measurements of dielectric properties during the imidization reaction have been described in section 3.2. The independent determination of the extent of reaction was carried out using FT-IR Spectroscopy. The procedure for and results of these experiments have been described in section 3.3.

An important point to be noted in the procedures for these two experiments is that the samples which underwent dielectric analyses had practically identical treatments and histories as those which underwent FT-IR spectroscopy. This situation was true for the soft-bake or solvent removal step as well as for the imidization schedule. Therefore, dielectric properties of the sample at any stage in the reaction can be correlated with the

extent of imidization. Figures 3.12-a, 3.13-a and 3.14-a are the plots of permittivity against degree of imidization at temperatures 130°C, 160°C and 200°C respectively. Figures 3.12-b, 3.13-b and 3.14-b show the change in loss factor as a function of imidization at these respective temperatures.

From the figures 3.12 through 3.14, it is noted that the permittivity and loss factor decrease as the extent of imidization increases at a particular temperature. The decrease is more significant at lower frequencies than at higher frequencies. This decrease can be attributed to the loss of polar units during imidization where the more polar amic acid-NMP complex gets converted to the less polar imide unit. Another reason for the decrease in the dielectric constant is that the molecules become more closely packed after imidization, thus rigidifying the system and reducing the mobility of the dipoles.

An additional point to be noted is that towards the end of the reaction at any temperature, the conversion increases by just a few per cent or has levelled off. However, the dielectric properties decrease monotonically, although very slightly. This indicates that the dielectric measurements are very sensitive to small changes in molecular structure.

Figures 3.15 through 3.17 are the plots of two runs at each of the three temperatures. The reproducibility is poor earlier during the imidization. This is due to the effect of atmospheric moisture that diffuses into the sample on the mobility of the ions in the sample. Thus, the extent of electrode polarization would be different for different samples. The permittivity is reproduced at all the three temperatures. One possible reason for the cause for the poor reproducibility in ε'' at 160°C is that on a log scale, the small differences in value get magnified for values less than 1. However, the percentage difference between the loss factor values is signigicant. No explanation is available for this behavior at this point.

From the plots of permittivity versus extent of imidization, it is noted that the permittivity decreases as the number of amic acid units being converted to imide units increases. The change in chemistry brings about a change in the dipole moment of the monomer units in the system. Closer investigation reveals that the dipole moment of the monomer units decreases due to imidization. The dielectric properties of the material also decrease due to imidization. It is therefore of interest to relate these two phenomena. Chapter 4 describes the development of the model to achieve this goal and the analysis of the model so developed. Earlier investigations {[Debye, 1929], [Onsager, 1936], [Frölich, 1958], [Smyth, 1930]} have attempted to relate the dielectric permittivity of a material to its dipole moment, and thus to its molecular structure. These previous investigations form the basis of the modelling presented in this study.

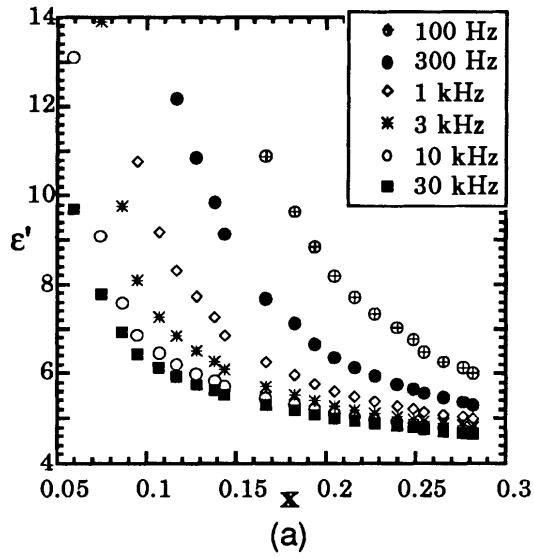

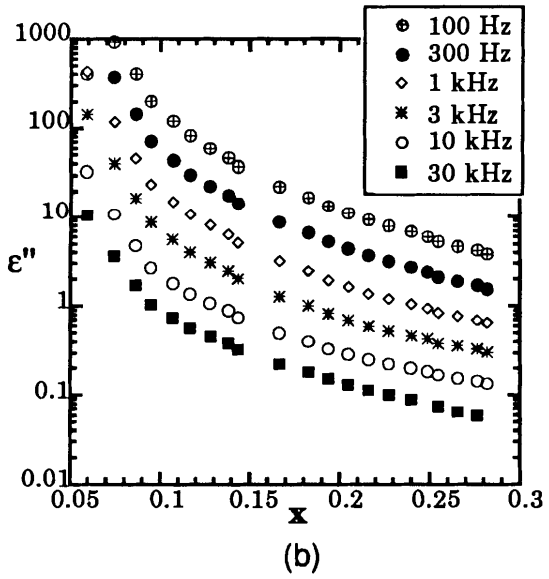

Figure 3.12: Dielectric properties as function of extent of imidization at 130°C:
(a) permittivity (b) loss factor.

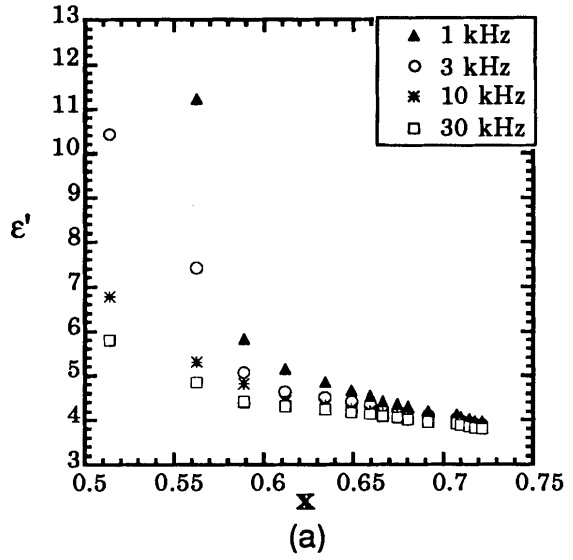

Figure 3.13: Dielectric properties as function of extent of imidization at 160°C:
(a) permittivity (b) loss factor.

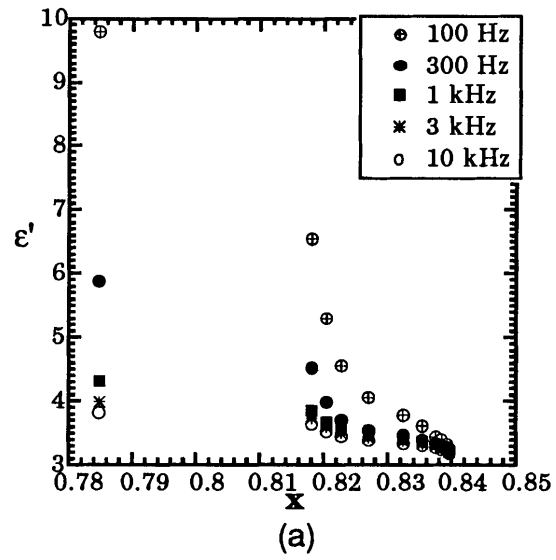

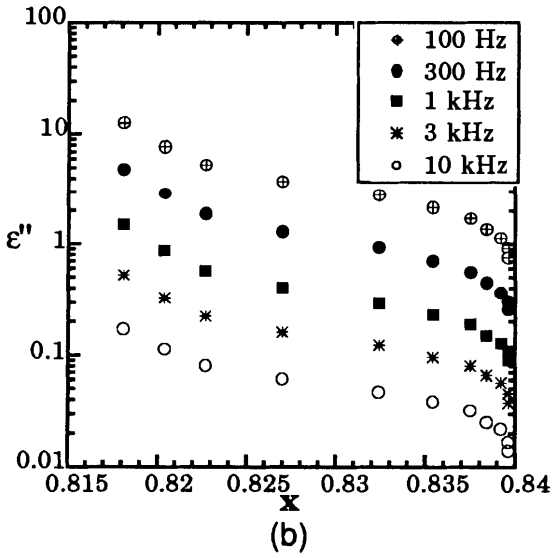

Figure 3.14: Dielectric properties as function of extent of imidization at 200°:
(a) permittivity (b) loss factor.

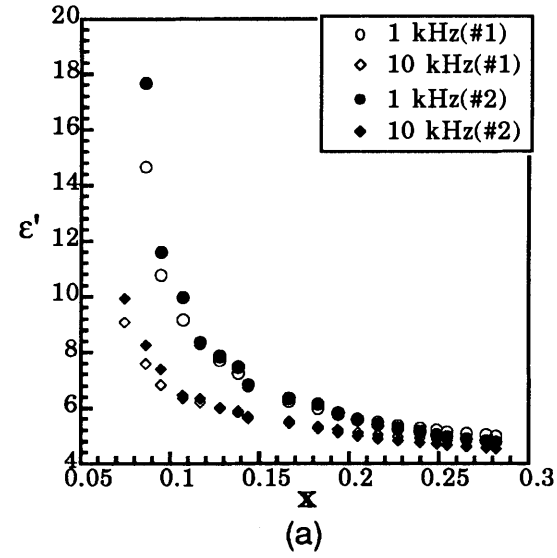

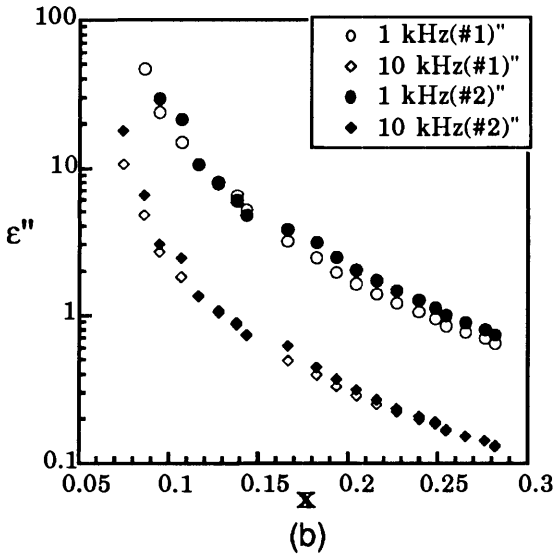

Figure 3.15: Dielectric properties as a function of extent of reaction for the experiments performed at 130°C: (a) permittivity (b) loss factor.

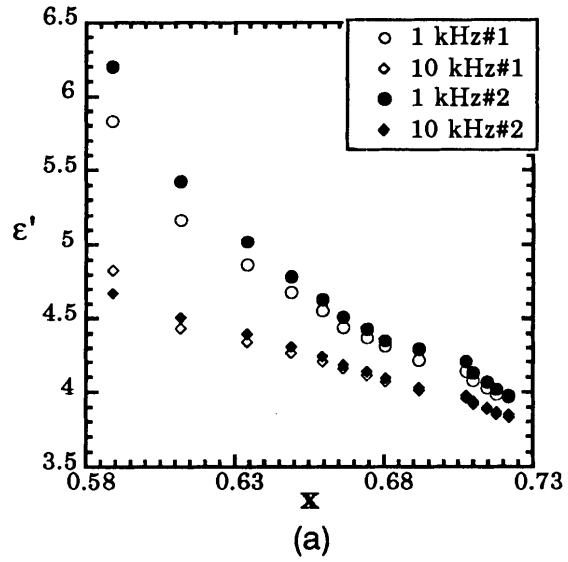

Figure 3.16: Dielectric properties as a function of extent of reaction for the experiments performed at 160°C: (a) permittivity (b) loss factor.

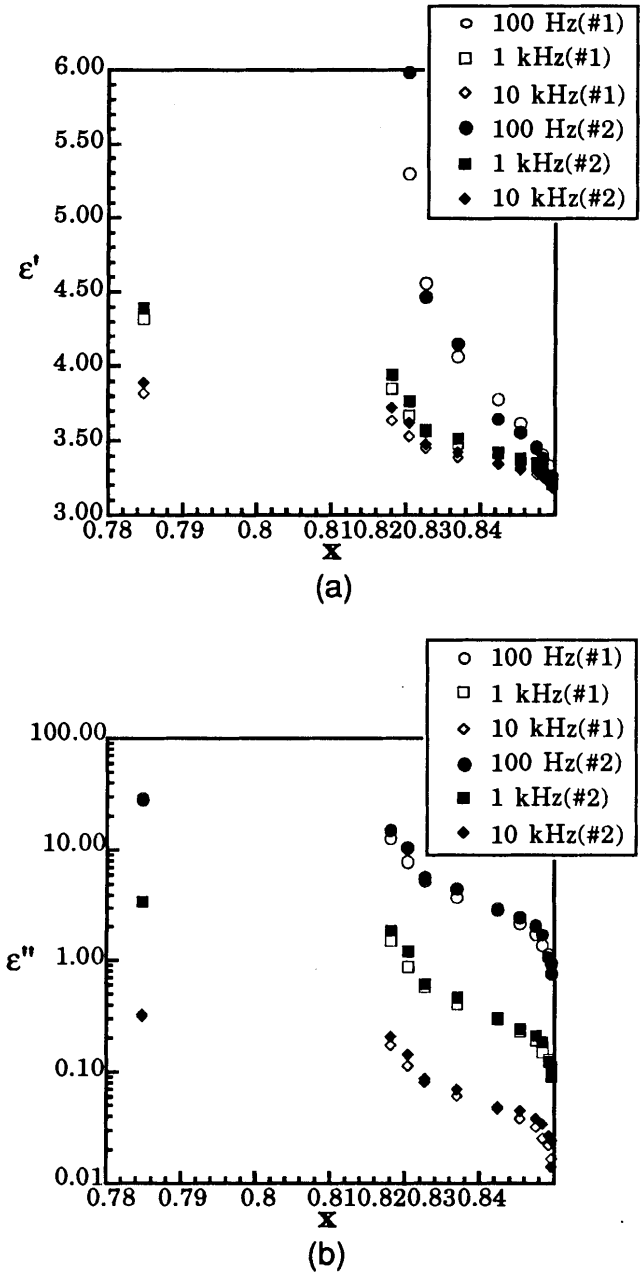

Figure 3.17: Dielectric properties as a function of extent of reaction for the experiments performed at 200°C: (a) permittivity (b) loss factor.

CHAPTER IV

ANALYSIS AND MODELLING OF EXPERIMENTAL RESULTS

4.1 Theoretical Modelling

This section presents the model development to relate dielectric properties to the chemistry. The dipole moment of a material depends on its molecular structure. The dielectric properties are related to this dipole moment. The theory to relate dielectric properties of a polar substance to its dipole moment has already been developed {[Debye, 1929], [Onsager, 1936], [Frölich, 1958], [Smyth, 1930]}. This theory was used to determine the relationship between the dielectric properties of homopolymers to the dipole moment of their repeat units [McCrum et al., 1967]. This investigation attempts to develop a model which relates the dielectric properties of a reactive polymer system to the chemistry by considering the dipole moments of the reactant and product monomer units.

To understand the theory of dielectric permittivity, the simplest case of a material made up of nonpolar, non-interacting molecules will be considered first. When one of these molecules is placed in an electric field, **E**, a dipole moment, **m**, is induced by the atomic and electronic polarizations. The dipole moment is directly proportional to the electric field and the proportionality constant is the deformation polarizability α_E [Debye, 1929].

$$\mathbf{m} = \alpha_E \mathbf{E} \qquad (4.1)$$

The deformation polarizability can be obtained from the Clausius-Mossotti relation [Solymar and Walsh, 1988] :

$$\frac{(\varepsilon_U - 1)}{(\varepsilon_U + 2)} = \frac{N_m \alpha_E}{3\varepsilon_0} \qquad (4.2)$$

In this expression, ε_U is the unrelaxed relative permittivity and is related to the polarization of atoms and electrons, which is independent of frequency; ε_0 is the permittivity of free space ($10^{-9}/36\pi$ Farad/m); N_m is the number of dipoles per unit volume.

From the Boltzman distribution of the orientation of the dipoles in an electric field, the mean dipole moment $\langle \mu \rangle$ of a polar gas of molecular dipole moment μ_0 is obtained from the expression [Solymar and Walsh, 1988]:

$$\langle \mu \rangle = \frac{\mu_0^2 \mathbf{E}}{3kT} \qquad (4.3)$$

k = Boltzman's constant = 1.38 x 10^{-23} J/°K/molecule

T = temperature (°K)

Hence, the orientation polarizability is:

$$\alpha = \frac{\mu_0^2}{3kT} \qquad (4.4)$$

Therefore, by replacing the atomic and electronic polarizability by an ensemble consisting of atomic and electronic polarizability and orientational polarizability, Debye (1929) obtained the relation:

$$\frac{(\varepsilon_R - 1)}{(\varepsilon_R + 2)} = \frac{N_m}{3\varepsilon_0}\left[\alpha_E + \frac{\mu_0^2}{kT}\right] \qquad (4.5)$$

Equation 4.5 is in terms of ε_R, the relaxed relative permittivity, (relative permittivity at very low frequencies) because, in addition to a dependance on atomic orientation, ε_R also depends on the orientation of molecules. This expression has been applied to polar gases at low pressure and also to dilute solutions of polar substances in nonpolar solvents [Debye, 1929].

Onsager (1936) developed an expression for the relaxed permittivity of liquids. In his analysis, Onsager considered the molecule to be a polarizable point dipole, at the center of a spherical cavity in a homogeneous medium having dielectric constant equal to ε_R. By considering the total field acting on the dipole to be the vector sum of the reaction field due to the dipole and the externally applied field, the following expression was obtained:

$$\frac{(\varepsilon_R - \varepsilon_U)(2\varepsilon_R + \varepsilon_U)}{\varepsilon_R(\varepsilon_U + 2)^2}(9\varepsilon_0 kT) = N\mu_0^2 \qquad (4.6)$$

Equation 4.6 is true only for non-interacting molecules and is not valid for liquids with strong intermolecular interactions like water and polymers, although this expression is successful for some simple polar molecules. In this expression, the α_E term is accounted

for by expressing it using the Clausius-Mossotti formula (equation 4.2). In equation 4.6, μ_0 is the dipole moment of the molecule, when the material is in the gaseous phase.

Kirkwood (1939) attempted to account for the interactions between neighboring dipoles. Unlike Onsager's assumption of a spherical cavity, Kirkwood assumed the sphere to be filled with interacting dipoles and obtained the expression:

$$\frac{(\varepsilon_R - 1)(2\varepsilon_R + 1)}{9\varepsilon_R}\frac{M}{d} = \frac{4\pi N}{3}\left[\alpha_E + \frac{g\mu^2}{kT}\right] \qquad (4.7)$$

In this expression, M is the molecular weight; d is the density; g is the correlation factor that quantifies the interactions of a reference dipole with neighboring dipoles; μ is the dipole moment of a molecule in the liquid phase. μ can alternatively be described as the dipole moment of a molecule when it is surrounded by a medium with relaxed relative permittivity of ε_R and unrelaxed relative permittivity (relative permittivity at high frequencies) of ε_U. The correlation factor g is expressed by:

$$g = 1 + z\overline{\cos\gamma} \qquad (4.8)$$

where, z is the number of nearest neighbors to the reference molecule and γ is the angle between the reference molecule and one of its z nearest neighbors. Kirkwood (1939) used statistical mechanics to develop this theory and empirically added the deformation polarization term, α_E. Consequently, this relation does not reduce to Onsager's relation (equation 4.6) for g=1. This equation has been successful only for materials for which $\varepsilon_R >> 1$ (i.e.water and some simple alcohols).

Frölich (1958) derived a general expression for the permittivity of a polar material. He accounted for the interaction between dipoles and reduced to Onsager's correlation for non-interacting dipoles, in which case the interaction correlation factor was unity. Like Onsager, he used the concept of two fields acting on a dipole: the reaction field due to the dipole and the external field. Additionally, he used the Clausius-Mossotti formula as an expression for the deformation polarizability. The resulting expression (modified to the MKS units) was :

$$\frac{(\varepsilon_R - \varepsilon_U)(2\varepsilon_R + \varepsilon_U)}{\varepsilon_R}(\varepsilon_0 kT) = N\overline{\mathbf{m}\mathbf{m}^*} \qquad (4.9)$$

This expression is for a material made up of polar units with dipole moment **m**. The term $\mathbf{m}^*$ is the dipole moment of a large spherical region embedded in its own medium polarized by one of its units which is in such a configuration that its dipole moment is **m**. $\mathbf{m}^*$ differs from **m** due to the existence of short-range forces or due to the non-spherical shape of the molecules. Also, in this expression, $\overline{\mathbf{m}\mathbf{m}^*}$ is the average value of the product $\mathbf{m}\mathbf{m}^*$ taking into account all the possible configurations and weighing them according to the probability of finding the unit in such a configuration.

At this point Frölich incorporated Kirkwood's theory of interactions between adjacent dipoles. If the unit is a polar molecule with dipole moment μ, then

$$\mathbf{m} = \mu \qquad (4.10)$$

Similarly,

$$\mathbf{m}^* = \mu^* \tag{4.11}$$

Also, since all dipolar directions are equivalent in a liquid, $\mu\mu^*$ will have the same value for all directions. Hence,

$$\overline{\mathbf{mm}^*} = \overline{\mu\mu^*} = \mu\mu^* \tag{4.12}$$

The right hand side term in equation 4.12 can be expressed as:

$$\mu\mu^* = g\mu^2 \tag{4.13}$$

In this equation, μ is the magnitude of the dipole moment of the polar molecule and g is the correlation factor.

Note that μ is related to μ_0 by the relation [Frölich, 1958]:

$$\mu = \frac{(\varepsilon_U + 2)}{3}\mu_0 \tag{4.14}$$

This leads to Frölich's modification of Kirkwood's formula (equation 4.7) [Frölich, 1958]:

$$\frac{(\varepsilon_R - \varepsilon_U)(2\varepsilon_R + \varepsilon_U)}{\varepsilon_R(\varepsilon_U + 2)^2}(9\varepsilon_0 kT) = Ng\mu_0^2 \tag{4.15}$$

N = number of molecules per unit volume

g = correlation factor for interaction between molecules

μ_0 = dipole moment of a molecule of the material in the gaseous phase

For a polymer [McCrum et al., 1967], the dipole moment μ_0 becomes,

$$\mu_0 = \sum_1^n p_k \qquad (4.16)$$

p_k = dipole moment of the k^{th} monomer repeat unit.

As a simplifying assumption, it is assumed that the dipole moments of all the repeat units are equal. For a high molecular weight polymer, the effect of the differences between the end groups and the polymer backbone repeat units can be neglected. This leads to [McCrum et al., 1967]:

$$\frac{(\varepsilon_R - \varepsilon_U)(2\varepsilon_R + \varepsilon_U)}{\varepsilon_R(\varepsilon_U + 2)^2}(9\varepsilon_0 kT) = N_r g'_r p_0^2 \qquad (4.17)$$

N_r = number of monomer repeat units per unit volume

p_0 = dipole moment of the monomer repeat unit if it were to exist in the gaseous phase.

g'_r = interaction parameter for a repeat unit in a polymer molecule.

In equation 4.7, g is the interaction parameter for a molecule and in equation 4.17 g'_r is the analogous term for a repeat unit in a polymer molecule. There are two ways to express g'_r for a polymer with n as the degree of polymerization [McCrum et al., 1967]:

(1) For the case of a dilute solution of distinct, monodisperse polymer molecules:

$$g'_r = 1 + \sum_{j=2}^{n} \left(\overline{\cos\gamma_{1j}} \right) \qquad (4.18)$$

γ_{1j} = angle between the reference unit 1 and the j^{th} unit in the same chain.

$\overline{\cos\gamma_{1j}}$ = value of the $\cos\gamma_{1j}$, averaged over the entire chain.

Comparing equation 4.18 with equation 4.8, the z term is replaced with the summation Σ sign. An assumption governing this expression is that all the units make an equal contribution to the value of $(g'_r - 1)$.

(2) For the case of entangled polymer molecules.

$$g'_r = 1 + \sum_{j=2}^{n} \left(\overline{{}^{I}\cos\gamma_{1j}} \right) + \sum_{j=1}^{n} \left(\overline{{}^{II}\cos\gamma_{ij}} \right) \qquad (4.19)$$

$\overline{{}^{I}\cos\gamma_{1j}}$ = average of the cosine of the angle between a reference unit 1 and a unit j within the same polymer chain. This term corresponds to intra-chain interactions.

$\overline{{}^{II}\cos\gamma_{ij}}$ = average of the cosine of the angle made between a reference unit i and a unit j which does not belong to the polymer chain that contains the reference unit i. This term corresponds to inter-chain interactions.

During the imidization of polyamic acid to polyimide, there are two kinds of dipoles:

(1) amic acid groups

(2) imide groups

Hence, instead of a single type of interaction between identical dipoles interacting, there are two kinds of dipoles giving rise to three different kinds of interactions. Therefore, if one considers the right hand side of equation 4.17, a modification of the term $g'_r \mathbf{p}_0^2$ is required to account for such a situation. The following modification is proposed for this study:

$$g'_r p_0^2 = \sum_{i=1}^{2}\sum_{j=1}^{2} g'_{r-ij} x_i x_j \mathbf{p}_i \mathbf{p}_j \qquad (4.20)$$

In this equation, x_i and x_j are the mole fractions of groups i and j respectively and $\mathbf{p}_i$ and $\mathbf{p}_j$ are the corresponding dipole moments in the gaseous phase. Here the subscripts i and j, each take values 1 and 2. The amic acid group will be denoted with the subscript 1 and the imide group will be denoted with the subscript 2. The justification for such a modification is that the term inside the summation sign on the right hand side of equation 4.20 is a general expression describing an interaction between components i and j multiplied by the probability that such an interaction will take place. The probability that component i interacts with component j is $x_i x_j$.

At a given time during the imidization process,

$$x_1 = (1\text{-}x) \qquad (4.21\text{-a})$$

$$x_2 = x \qquad (4.21\text{-b})$$

where, x is the degree of imidization at this time.

From equations 4.17, 4.20, 4.21-a and 4.21-b, the resulting expression obtained is:

$$\frac{(\varepsilon_R - \varepsilon_U)(2\varepsilon_R + \varepsilon_U)}{\varepsilon_R(\varepsilon_U + 2)^2}\frac{(9\varepsilon_0 kT)}{N_r} = g'_{r-11}(1-x)^2\mathbf{p}_1^2 + g'_{r-22}x^2\mathbf{p}_2^2 + 2g'_{r-12}(1-x)x\mathbf{p}_1\mathbf{p}_2 \quad (4.22)$$

To estimate g'_r, one needs to be able to determine the average cosine of the angle between two monomer units - within the same chain or in two different chains. For this, one needs to have the Boltzman distribution function. From Frölich (1958), the following Boltzman distribution function is obtained.

$$\overline{\cos\gamma} = \frac{\int \cos\gamma \exp\left(-U/kT\right) d\omega_1 d\omega_2}{\int \exp\left(-U/kT\right) d\omega_1 d\omega_2} \quad (4.23)$$

U	=	energy of interaction between neighboring molecules
$d\omega_1, d\omega_2$	=	surface elements of the solid angles of the directions of the two dipoles.

Generally, U can be an even or an odd function of cosγ. Hence, it can be expressed as:

$$U = U_{even} + U_{odd} \quad (4.24)$$

Hence, if $|U_{odd}| \ll kT$, then,

$$\overline{\cos\gamma} = \frac{-U_0}{kT} \tag{4.25}$$

In this equation [Frölich, 1958],

$$U_0 = \frac{\int \exp\left(-U_{even}/kT\right) U_{odd} \cos\gamma \, d\omega_1 d\omega_2}{\int \exp\left(-U_{even}/kT\right) d\omega_1 d\omega_2} \tag{4.26}$$

For the imidization of polyamic acid to polyimide, most of the solvent has been removed at the onset of reaction. Hence, the entangled polymer expression (equation 4.19) is to be used for g'_r. This assumes that both intra-chain and inter-chain interactions exist between monomer repeat units. Since the expression for g'_r contains 2n-1 cosine terms, its value is bound between 2-2n and +2n. To obtain an equation in terms of energy, let:

$$-zU_{o\text{-}11} = kT(g'_{r-11} - 1) \tag{4.27-a}$$

$$-zU_{o\text{-}22} = kT(g'_{r-22} - 1) \tag{4.27-b}$$

$$-zU_{o\text{-}12} = kT(g'_{r-12} - 1) \tag{4.27-c}$$

In equations 4.27-a, 4.27-b and 4.27-c, $U_{o\text{-}ij}$ are the interaction energies between species i and j; z is the number of nearest neighbors and its value is 2n-1.

From equations 4.17, 4.22, 4.27-a, 4.27-b, 4.27-c, the final expression becomes:

$$\frac{(\varepsilon_R - \varepsilon_U)(2\varepsilon_R + \varepsilon_U)}{\varepsilon_R(\varepsilon_U + 2)^2}(9\varepsilon_0 kT) = N_r\left[\left(1 - \frac{U_{0\text{-}11}}{kT}\right)(1-x)^2 p_1^2 + \left(1 - \frac{U_{0\text{-}22}}{kT}\right)x^2 p_2^2 + 2\left(1 - \frac{U_{0\text{-}12}}{kT}\right)(1-x)x p_1 p_2\right] \quad (4.28)$$

To facilitate the study of the imidization reaction, the following assumptions are made:

(1) No water, aromatic hydrocarbon solvent, or free (non-complexed or unbound) NMP is present in the film after the pre-bake step.

Carried out prior to the imidization, the pre-bake step is at a temperature that is high enough (100°C) to evaporate the volatiles (i.e. condensed moisture) and a significant portion of the solvent, but the temperature is not high enough to allow any significant part of the imidization to take place. This is a simplification, because, in practice, imidization begins at temperatures above 4°C [Soane and Martynenko, 1989]. However, from the FT-IR analysis of the sample after the 1 hour pre-bake at 100°C, it was noted that no imidization was discernible. This meant that the extent of reaction was less than 2% (the lowest extent of imidization that was measurable during the reaction carried out at 130°C in the present investigation).

(2) During imidization, two NMP molecules are complexed with every amic acid repeat unit.

This assumption is justified because, Brekner and Feger (1987) performed thermogravimetric analyses and observed that initially, all the unbound NMP evaporated in the pre-bake step (this pre-bake involved heating in air, at 80°C, on a hot plate for 30 minutes). At this point, 4 NMP molecules were bound to each amic acid group. On

continuing the pre-bake, the loosely bound 2 NMP molecules per amic acid unit decomplexed, leaving 2 NMP molecules complexed with each amic acid group. This was further confirmed by Simoff et al. (1990) who performed the pre-bake at 100°C for one hour.

(3) At the end of imidization, all the NMP has been removed.

Almost complete imidization takes place at temperatures of 300°C to 420°C {[Pryde, 1989-b], [Soane and Martynenko, 1989]}, which are well above the boiling point of NMP (about 202°C) [Aldrich, 1990]. On complete imidization, there are no more sites where the NMP can be complexed. However, this is a simplification, because imidization is never 100% complete, but is assumed to be so for all practical purposes when no more weight loss is observed. In addition, some of the NMP molecules might remain in the material at the end of imidization because of the increased resistance to diffusion due to imidization. There probably are trace quantities of NMP in the final sample. However, in this study, this small amount of NMP will be neglected.

(4) No thermal degradation or side reactions occur.

The imidization reaction is carried out at temperatures below the degradation temperature (~ 450°C) for the polyimide . This assumption is supported by Pryde (1989-b), who found no evidence of noncyclic imide crosslinks and isoimide formation in the FT-IR study of imidization at temperatures above 200°C. Brekner and Feger (1987) have also stated that no anhydrides had been detected in films of fully imidized PMDA-ODA polyimide because imide formation is thermodynamically more favorable than anhydride formation.

(5) Throughout the imidization, NMP and water are assumed to evolve in the ratio 1:1.

This assumption is made because two water molecules are evolved as an amic acid group imidizes. Due to the imidization, decomplexation of the NMP molecules from the amic acid units on the chain occurs due to the loss of active sites. This is only an assumption because earlier investigations [Simoff et al., 1990] showed that NMP and water were evolved in the ratio 1.3±0.2:1 over the temperature range 110°C-270°C. The decomplexation of NMP and the subsequent evaporation proceeds even when the reaction has slowed down significantly. However, it is necessary to make this simplifying assumption so that the dipole moment of an amic acid-NMP complex unit can be considered to be constant during imidization because the number of NMP molecules complexed with each amic acid unit would then be constant.

The next step is the determination of N_r (the number of repeat units per unit volume). To achieve this, the following data are needed:

Density of the solution	= 1.097g/cc [Du Pont , 1989]
Weight fraction polyamic acid	= 0.159 [Du Pont , 1989]
Weight fraction NMP	= 0.841 [Du Pont , 1989]
Density of Pure NMP	= 1.033g/cc [Aldrich, 1990]
Density of fully imidized polyimide	= 1.42g/cc [Du Pont, 1988]

Hence, density of polyamic acid can be calculated from the preceding information.

Density of fully imidized polyamic acid	= 1.4355g/cc

To convert the densities to N_r one needs the formula weights of the groups involved.

Formula weight of an amic acid group = 446

Formula weight of imide group = 410

Formula weight (FW) of NMP = 99

Since two NMP molecules are bound to each amic acid repeat unit, then the weight fraction of polyamic acid in the sample at the onset of imidization is

$$\frac{FW_{amic\ acid}}{FW_{amic\ acid} + 2(FW_{NMP})} = 0.693.$$

The density of the polyamic acid - NMP complex is calculated to be 1.312g/cc. and the bulk density of the polyamic acid in this sample then is 0.9084g/cc.

To convert density to repeat units/m^3, the procedure is to divide the density in kg/m^3 by the formula weight and multiply by Avogadro number. Thus at the beginning of imidization,

N_r = 1.227×10^{27} repeat units/m^3 is obtained.

From the density of fully imidized polyimide,

N_r = 2.086×10^{27} repeat units/m^3 is obtained as the N_r for fully imidized polyimide.

During the imidization,

$$N_r = N_{r1}(1-x)+N_{r2}x \qquad (4.29)$$

N_{r1} = N_r of the polyamic acid-NMP complex

= 1.227 x 10^{27} amic acid units/m^3

N_{r2} = N_r of the polyimide fraction

= 2.086 x 10^{27} imide units/m^3

x = Degree of imidization

N_{r1} and N_{r2} are intrinsic group densities of the two materials. Since these quantities depend on temperature, they are both constant throughout isothermal imidization.

$U_{0\text{-}ij}$ values are assumed to remain constant during imidization because they depend on the nature of the interacting species. The system can be considered to be a binary mixture of amic acid groups and the imide groups. The concentrations or quantities of these groups change during imidization. The moment $\mathbf{p}_2$ is taken to be equal to the dipole moment of diphenyl ether, which is 1.0 Debye [Smyth, 1930].

The left hand side of equation 4.28 was determined from the microdielectrometric measurements. On the right hand side, x can be obtained from the FT-IR spectroscopy measurements. From the dielectric properties of fully imidized polyimide as a function of frequency, g'_{r-22} can be determined. The terms $(g'_{r-11}\,\mathbf{p}_1^2)$ and $(g'_{r-12}\,\mathbf{p}_1)$ can be determined by fitting equation 4.22.

It is impossible to determine $\mathbf{p}_1$ from structure in the way $\mathbf{p}_2$ was determined because there are many degrees of freedom and the polar segments can be vectorially added in numerous ways. There is no data available in the form of Boltzman's distribution function to determine the most probable or the average dipole moment of the amic acid group. Hence a best fit was required for the parameters $(g'_{r-11}\,\mathbf{p}_1^2)$ and $(g'_{r-12}\,\mathbf{p}_1)$. The dipole moments in the gaseous phase, $\mathbf{p}_1$ and $\mathbf{p}_2$, being reference values, are invariant with temperature. The interaction parameter g'_r does vary with temperature. However, it is

assumed to remain constant during isothermal imidization. Hence, the best fits were taken over the imidization reactions at each of the three temperatures (130°C, 160°C and 200°C).

4.2 Analysis of Experimental Results

4.2-1 Determination of relaxed and unrelaxed premittivities

The left hand side of the model (equation 4.28) contains terms that are to be determined from dielectric measurements. It is therefore necessary to extract the limiting low and high frequency values from the frequency response of the material undergoing dielectric analysis. The relaxed permittivity ε_R is the limiting value of ε' at low frequencies and the unrelaxed permittivity ε_U is the limiting value of ε' at high frequencies. However, as the frequency decreases, the permittivity has been observed to increase without levelling off (figure 3.5). This effect can be attributed to electrode polarization as described in section 2.1-3. Hence, the data considered for analysis should be in the regime where electrode polarization is not dominant. As seen in figure 3.5-b, the slope of the plot of ε'' versus frequency is -1 even in the range of frequencies greater than 10 kHz. This indicates that ionic conductivity dominates the loss factor in the earlier stages of the imidization. Additionally, ε'' is greater than ε' for frequencies up to 10 kHz, which indicates the significance of electrode polarization on the measured value of ε'. It is necessary to determine a frequency range such that the frequencies are large enough to have a minimal effect of electrode polarization on the measured values for a significant duration of the reaction. Hence, it is necessary to only consider dielectric properties in the region where measured ε'' is less than ε' [Sheppard, 1986], i.e. where the capacitative response is more

dominant than the conductive response. Since the upper limit of the frequency range for the System III Microdielectrometer is fixed at 100 kHz, the lower limit should be low enough to provide enough frequencies at which to measure the dielectric properties. Therefore, the data considered for analysis is only from that time during the imidization when the value of ε'' at 1 kHz is less than the corresponding ε'. The lower limit of 1 kHz was chosen because ionic conductivity was seen to dominate the value of ε'' for frequencies below and up to 1 kHz for significant durations of the imidization reactions at 130°C, 160°C and 200°C.

As described in the following paragraphs, the determination of ε_R and ε_U involves the determination of the losses due to dipole orientation. As seen in equation 2.15, ionic conductivity also contributes to loss factor. This effect has to be determined, and subtracted from the overall loss factor. The conductivity contribution to ε'' dominates at low frequencies, less than 1 kHz. Thus, in the plot of $\log_{10}(\varepsilon'')$ vs $\log_{10}(\omega)$, a straight line is observed in this frequency range. The ionic conductivity is extracted by considering the relationship described in equation 4.30 in this region.

$$\varepsilon'' = \frac{\sigma}{\omega \varepsilon_0} \qquad (4.30)$$

In this equation, ω is the angular velocity, which is 2π times the frequency, σ is the ionic conductivity in $1/\Omega m$ and ε_0 is the permittivity of free space. The ionic conductivity is thus determined for all the points lying on the straight line and the average is taken as the actual value. This ionic conductivity is subtracted from the ε'' data at higher frequencies.

When one plots this corrected dipole loss, ε'', against ε' on a linear scale, one obtains the values of ε_R and ε_U by extrapolating the curve joining the ε'' points to meet the ε' axis ($\varepsilon''=0$) at both the high permittivity end and the low permittivity end, respectively.

This is described in the following paragraphs. Usually, the curve will not tend to show a maximum, but just show a monotonic variation. In that case, it is necessary to use correlations between ε" and ε' to determine ε_R. In this investigation, two methods have been used.

The first method is based on Debye's analysis for the expression of the complex dielectric constant. In this method, one considers the loss factor as defined in equation 2.14. Ideally, this plot will be a semicircle with center at $((\varepsilon_R+\varepsilon_U)/2, 0)$ and a radius of $(\varepsilon_R - \varepsilon_U)/2$. Thus, the intercepts of the semicircle will be ε_U and ε_R. This can be proven by considering the equation of the circle in terms of equations 2.13 and 2.14 for ε' and ε" respectively:

$$\left[\varepsilon' - \frac{1}{2}(\varepsilon_R - \varepsilon_U)\right]^2 + \varepsilon''^2$$
$$= \frac{(\varepsilon_R - \varepsilon_U)^2}{4}\frac{(1-\omega^2\tau_d^2)^2}{(1+\omega^2\tau_d^2)^2} + \frac{(\varepsilon_R - \varepsilon_U)^2\omega^2\tau_d^2}{(1+\omega^2\tau_d^2)^2}$$
$$= \frac{(\varepsilon_R - \varepsilon_U)^2}{4} \qquad (4.31)$$

This method assumes a single relaxation time for the entire system; therefore, it is used for determining the values for the fully imidized Kapton® polyimide film, in which only one type of dipole (that of the diphenyl ether moiety) exists.

Most materials exhibit a distribution of relaxation times. In such cases, the points on a ε" vs ε' plot will lie within the semicircle. There have been various empirical correlations to describe such behavior.

$$\varepsilon^*(\omega) = \varepsilon_U + \frac{\varepsilon_R - \varepsilon_U}{(j\omega\tau_d)^\beta + 1} \qquad (4.32)$$

[Cole and Cole, 1941]

$$\varepsilon^*(\omega) = \varepsilon_U + \frac{\varepsilon_R - \varepsilon_U}{(j\omega\tau_d + 1)^\beta} \qquad (4.33)$$

[Davidson and Cole, 1950]

$$P(t) = \exp\left(\left[{}^{-t}/_{\tau_d}\right]^\beta\right) \qquad (4.34)$$

{[Williams and Watts, 1970], [Williams et al.,1971]}

In equations 4.32 and 4.33, ε^* is the complex dielectric constant. In equation 4.34, P(t) is the polarization function expressed by a non-exponential decay function. In each of the three equations, β is a distribution parameter for the relaxation times. The mean of these relaxation times is denoted by τ_d.

Though all three correlations are empirical in nature, there have been attempts to interpret the correlation by Williams and Watts in terms of relaxation based on diffusion {[Montroll and Bendler, 1984], [Shlesinger, 1984]}. The correlation by Davidson and Cole, which is easier to analyze, results in values that are very close to those values obtained by using the Williams and Watts function [Lindsay and Patterson, 1980]. Hence, the Davidson-Cole method was used in the analysis of the dielectric data during the imidization. It is necessary to consider a distribution of relaxation times during the imidization because of the presence of amic acid units in the system. Amic acid units are composed of more than one kind of polar group, which would have different relaxation times.

The complex dielectric constant, as expressed by equation 4.33 is broken into its real and imaginary parts as:

$$\varepsilon' = \varepsilon_U + \frac{(\varepsilon_R - \varepsilon_U)\cos(\beta\phi)}{\left(1+(\omega\tau_d)^2\right)^{\beta/2}} \tag{4.35}$$

$$\varepsilon'' = \frac{(\varepsilon_R - \varepsilon_U)\sin(\beta\phi)}{\left(1+(\omega\tau_d)^2\right)^{\beta/2}} \tag{4.36}$$

where,

$$\phi = \tan^{-1}(\omega\tau_d) \tag{4.37}$$

from equations 4.35 and 4.36 one obtains

$$\tan(\beta\phi) = \frac{\varepsilon''}{\varepsilon' - \varepsilon_U} \tag{4.38}$$

$$\tan\left(\frac{\pi}{2(\beta+1)}\right) = \omega_{max}\tau_d \tag{4.39}$$

In equation 4.39, ω_{max} corresponds to the frequency at which the ε'' is a maximum. On solving equations 4.38 and 4.39 simultaneously at a frequency at which ε'' is a maximum, it is possible to determine β and τ_d for each frequency scan during the imidization. Since ε_U is obtained directly from the data, it is sufficient to determine (ε_R-ε_U). ε_U is the high frequency permittivity at which ε'' is zero. If ε'' at the highest frequency is not zero, then ε_U

is determined by linearly extrapolating ε' against ε" till ε" becomes zero. (ε_R-ε_U) is then fitted in equation 4.40, which is obtained by combining equations 4.35 and 4.36.

$$(\varepsilon' - \varepsilon_U)^2 + \varepsilon''^2 = \frac{(\varepsilon_R - \varepsilon_U)^2}{\left(1 + (\omega\tau_d)^2\right)^\beta} \qquad (4.40)$$

Figures 4.1 through 4.3 illustrate some sample correlations between ε" and ε' during imidization reactions at 130°C, 160°C and 200°C respectively along with the Davidson-Cole fits as described above. The values of ε_R and ε_U are tabulated in the appendix for isothermal imidization reactions at each of the three temperatures.

4.2-2 Analysis of fully imidized Kapton® polyimide film

In equation 4.22, the right hand side contains three interaction parameters - g'_{r-11}, g'_{r-22} and g'_{r-12}. These three parameters and the dipole moment of an amic acid unit, $\mathbf{p}_1$ are the only unknown terms in that equation. These values can be determined by fitting. However, the number of fitted parameters can be reduced if one or more of these parameters can be determined experimentally. It is possible to determine the interactions between imide units by determining the dielectric properties of fully imidized polyimide film, which is available commercially. The dielectric data on fully imidized polyimide is described in section 3.4. This data is converted into ε_R and ε_U using the Debye analysis described in section 4.2-1. For fully cured polyimide, (1-x) equals zero. Since $\mathbf{p}_2$ is 1D, g'_{r-22} can be determined directly using the ε_R and ε_U data in equation 4.22. The loss factor is very close to zero and increases as the frequency increases. The frequency required to determine ε_U is greater than 100 kHz, the highest frequency that can be achieved by the

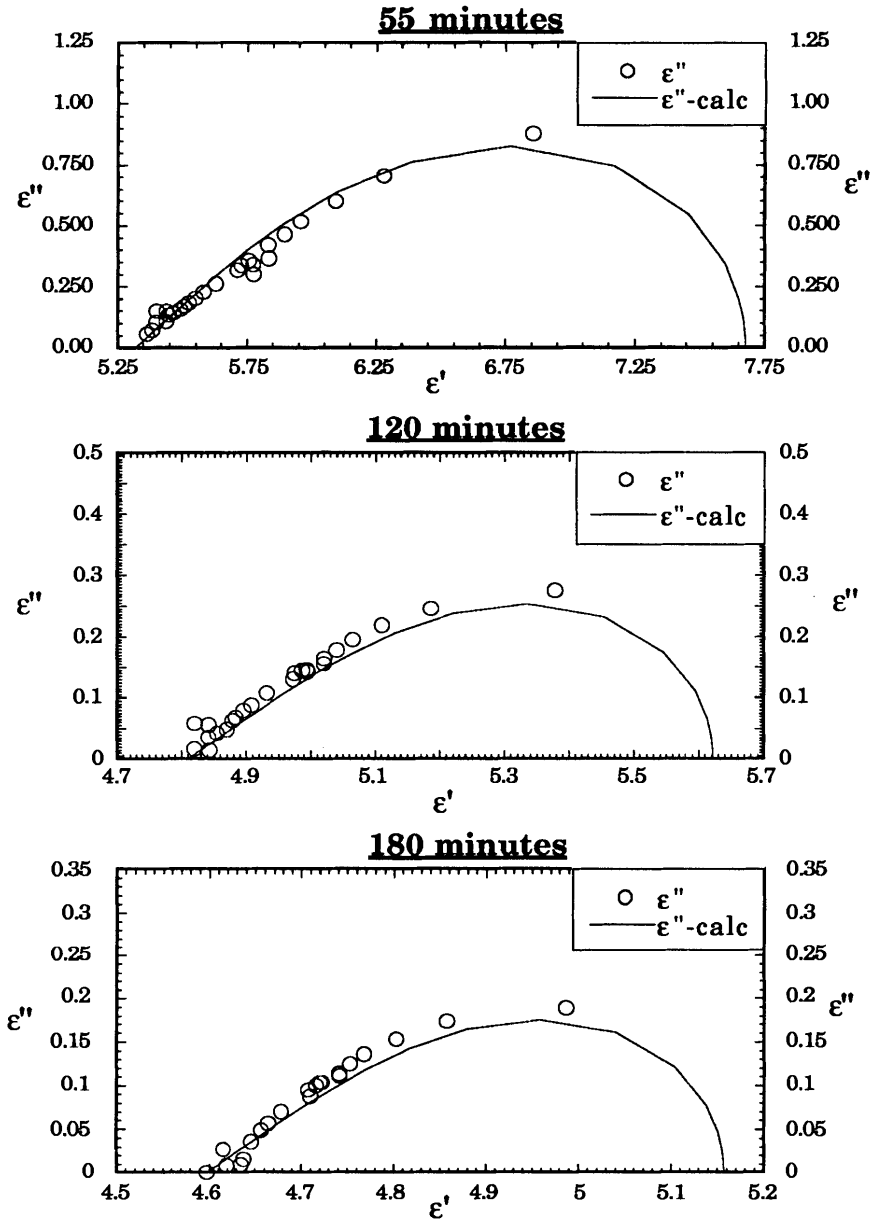

Figure 4.1: Davidson-Cole plots of dielectric properties during imidization at 130°C.

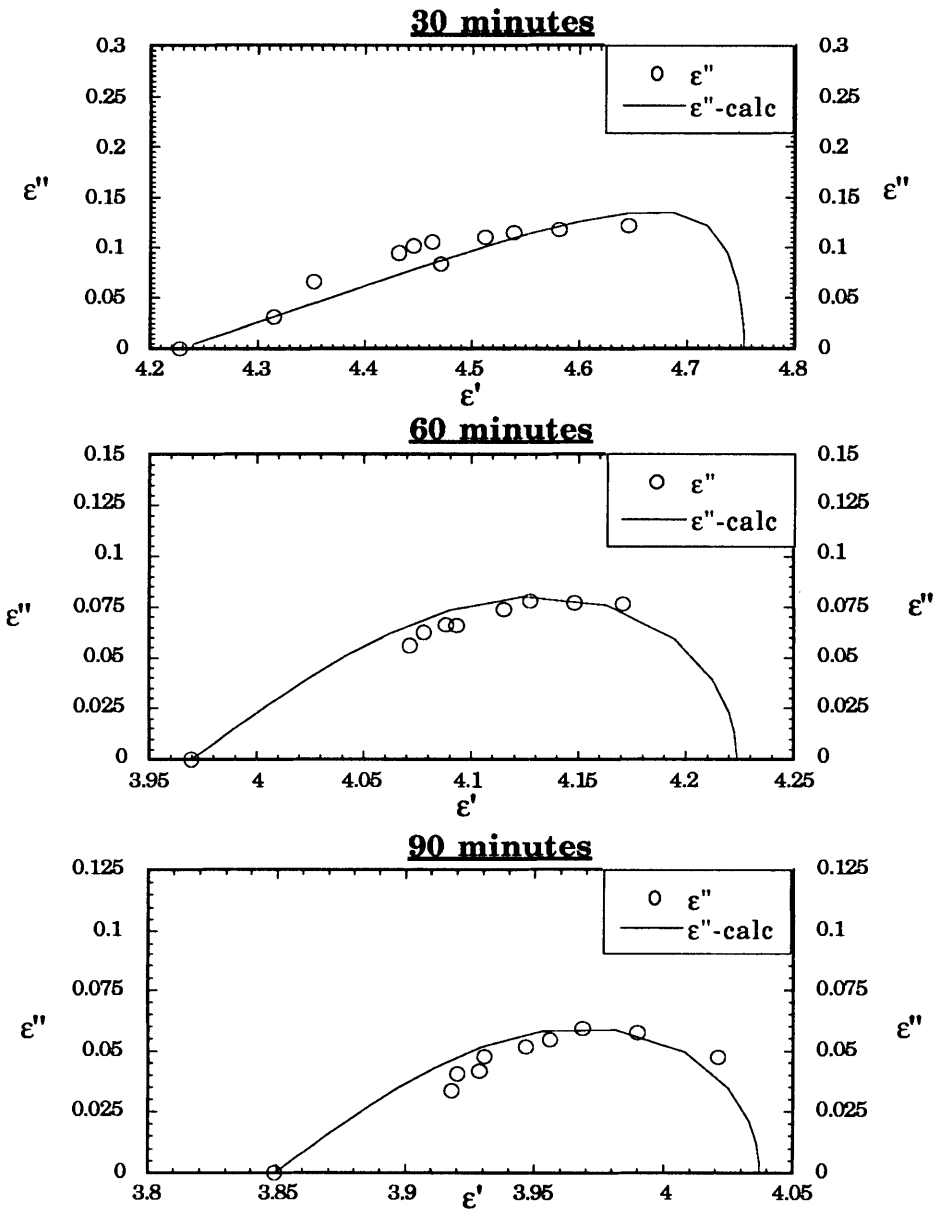

Figure 4.2: Davidson-Cole plots of dielectric properties during imidization at 160°C.

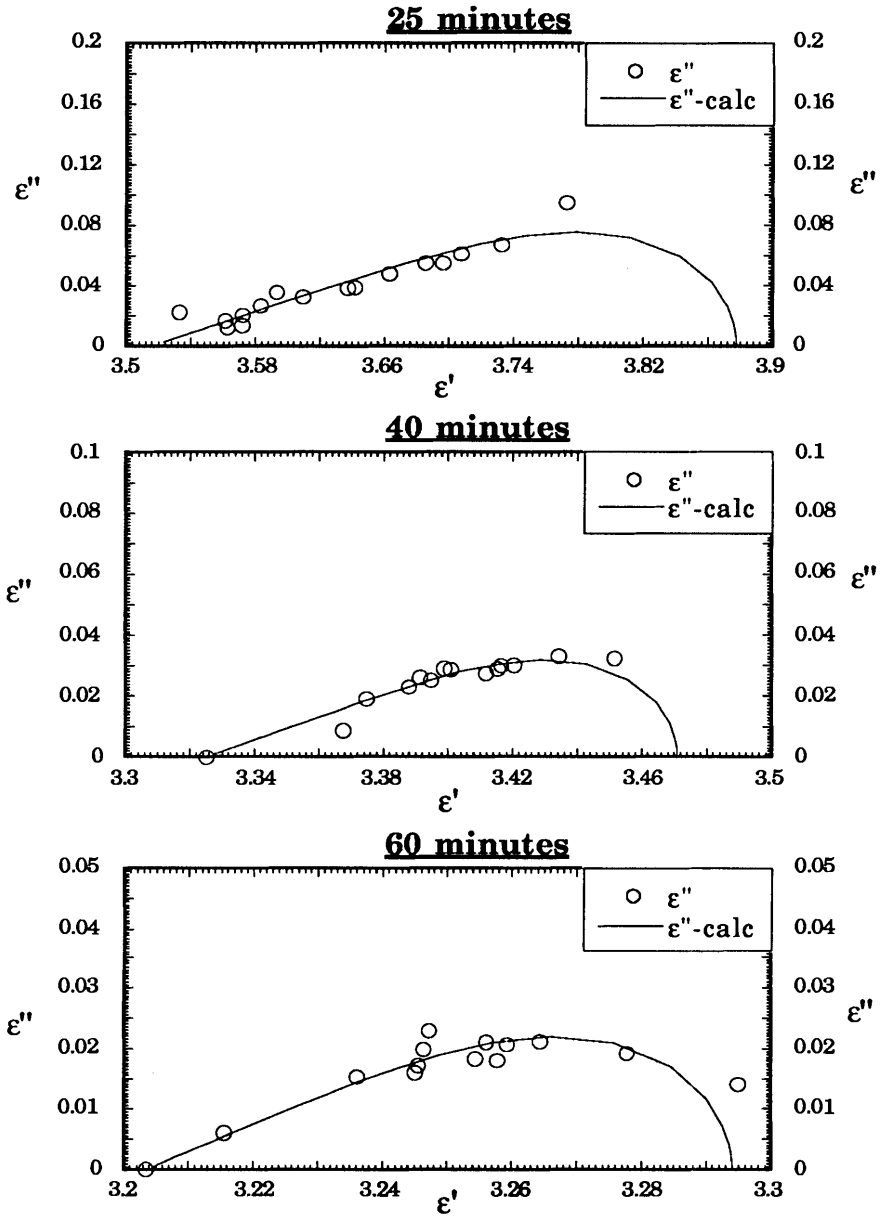

Figure 4.3: Davidson-Cole plots of dielectric properties during imidization at 200°C.

microdielectrometer. At 200°C, there is a decrease in loss factor as the frequency is increased. This could be because ionic conductivity dominates the loss factor in this region and ε'' can be expressed as in equation 4.30. The loss factor shows a minimum at about 1 kHz, above which ε'' increases with increase in frequency. Hence, only data at frequencies greater than the frequency of minimum loss is considered for analysis.

Figures 4.4 through 4.7 show the best fit Cole-Cole plots for fully imidized Kapton® films at 20°C and at each of the three respective reaction temperatures. It is observed that the best fit to the Debye relationship is very poor in the case of fully imidized polyimide film. This is attributed to the fact that the sensitivity of the instrument in terms of the loss factor is of the order of magnitude of the loss factor of the material. Also, the variation in ε' over the frequency range (~ 0.07) is about the same order of magnitude as its sensitivity (~0.01). The most probable reason for the poor fit is the assumption of a single relaxation time for the polyimide. It was not feasible to use the Davidson-Cole or any other available relationship to fit for dielectric properties of Kapton® film. This is because the determination of ε_U and ε_R involves the non-linear fitting for three parameters - τ_d, β and ε_U. The best fit values are strongly dependant on the initial guesses for the parameters. Hence, in spite of its disadvantages, Debye's relationship was used to determine ε_U.

The interaction parameter for Kapton® film, g'_{r-22} is determined by applying equation 4.22 and putting x=1. Table 4.1 lists the values of ε_R, ε_U and the g'_{r-22} interaction parameter at four temperatures, 20°C, 130°C, 160°C and 200°C at which the parallel plate measurements were carried out. There is no discernible trend in the g'_{r-22} values. The parameter has a lower value at 130°C than at 20°C. This behavior has not been properly understood. The values from 130°C to 200°C are in increasing order and are greater than the values at the lower temperatures. With rise in temperature, the mobility of the dipoles in the system increases. This should improve the alignment of the dipoles, corresponding to

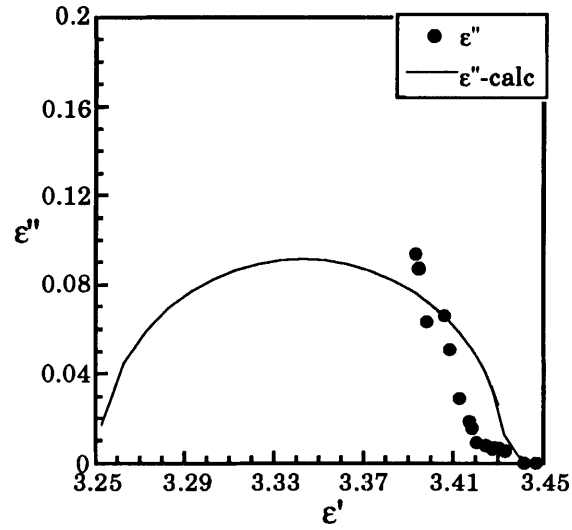

Figure 4.4: Cole-Cole plot (Debye's relationship) of dielectric measurements on fully imidized Kapton® film at 20°C.

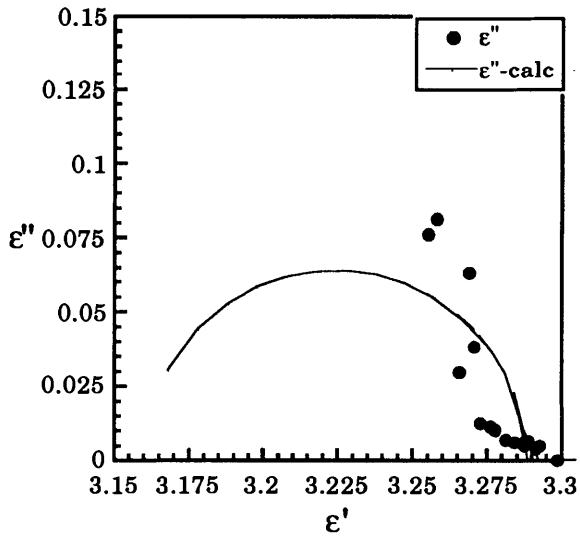

Figure 4.5: Cole-Cole plot (Debye's relationship) of dielectric measurements on fully imidized Kapton® film at 130°C.

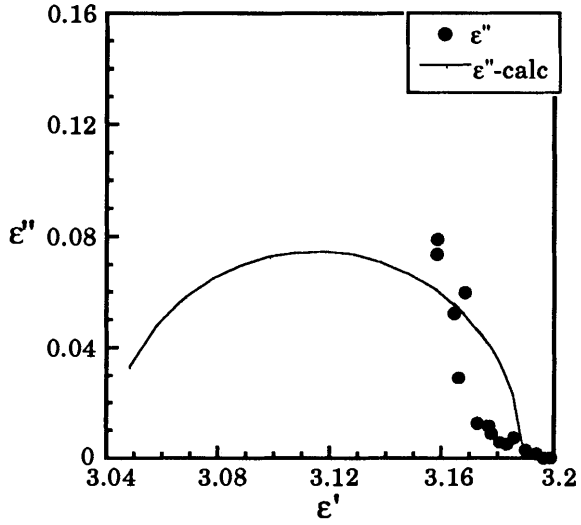

Figure 4.6: Cole-Cole plot (Debye's relationship) of dielectric measurements on fully imidized Kapton® film at 160°C.

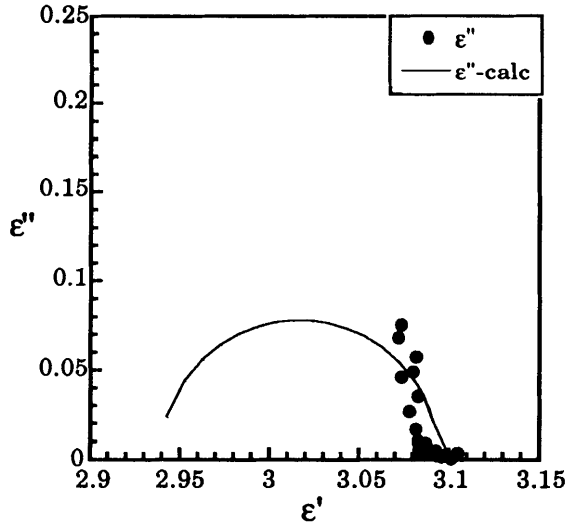

Figure 4.7: Cole-Cole plot (Debye's relationship) of dielectric measurements on fully imidized Kapton® film at 200°C.

an increase in (ε_R-ε_U), which would cause an increase in the interaction parameter. It should be noted that these values could be affected by the higher moisture content of the film at lower temperatures. However, determination of g'_{r-22} is necessary to reduce the number of fitted parameters in equation 4.22 from 3 to 2.

No trend can be inferred in the g'_{r-22} values because of a very large standard deviation. Hence, the effect of temperature on the orientation of dipoles cannot be determined. The quantity (ε_R-ε_U) indicates the effect of the orientation of all dipoles and this significantly affects the value of the parameter g'_{r-22}. However, as observed in table 4.1, the term does not show a significant variation over the temperature range from 20°C to 200°C. This implies that the temperature difference does not significantly affect the mobility of the dipoles. This behavior is not reasonable. It has been attributed to be largely due to the problems caused by the decrease in the moisture content of the film as the temperature is increased. Additionally, significant error is possible in the determination of ε_U and ε_R, because the variation of the measured permittivity values between samples at one frequency is greater than the variation over a frequency range for a single sample.

Table 4.1: Interaction parameter of fully imidized polyimide Kapton® as a function of temperature.

T°C	ε_R	ε_U	(ε_R-ε_U)	g'_{r-22}	std.dev(g'_{r-22})
20	3.4343	3.2517	0.1826	0.2694	0.0494
130	3.2883	3.1606	0.1277	0.2517	0.0202
160	3.1894	3.0412	0.1482	0.3676	0.0152
200	3.0950	2.9400	0.1550	0.5335	0.0772

4.2-3 Modelling Analysis of Dielectric measurements during imidization.

The relaxed and unrelaxed permittivities were determined using the method described in section 4.2-1 for the frequency scans during the imidization reactions at 130°C, 160°C and 200°C. The model being fitted is expressed in equation 4.41. The left hand side of the equation describes the points determined from the dielectric measurements. The right hand side is the curve that is generated by determining the best fit of the model parameters. The extent of reaction x was determined using FT-IR spectroscopy. From equation 4.29, N_T=1.227+0.859x (10^{27} units/m^3) is obtained. The values of g'_{r-22} at the different reaction temperatures were obtained from the parallel plate dielectric measurements of fully imidized polyimide film as described in section 4.2-2.

$$\frac{(\varepsilon_R-\varepsilon_U)(2\varepsilon_R+\varepsilon_U)}{\varepsilon_R(\varepsilon_U+2)^2}\frac{(9\varepsilon_0 kT)\left(10^{-27}\right)}{(1.227+0.859\ x)}\left(\frac{1\ D}{(3.364)\left(10^{-30}\ C-m\right)}\right)^2 - g'_{r-22}x^2p_2^2$$
$$= g'_{r-11}(1-x)^2p_1^2 + 2g'_{r-12}(1-x)xp_1p_2 \qquad (4.41)$$

The plots showing the best fits are illustrated in figures 4.8 through 4.10. As can be observed from the figures, the description of the system by the model is fair at 160°C and 200°C. The fit for imidization at 130°C shows less curvature than the data. The possible reasons for this kind of behavior are:

(1) Limitations of the Model:

It is possible that the model presented does not effectively describe the system. The simplifying assumption of NMP and water molecules evolve in the ratio 1:1 throughout the imidization could be giving rise to the poor fit at 130°C. Since the

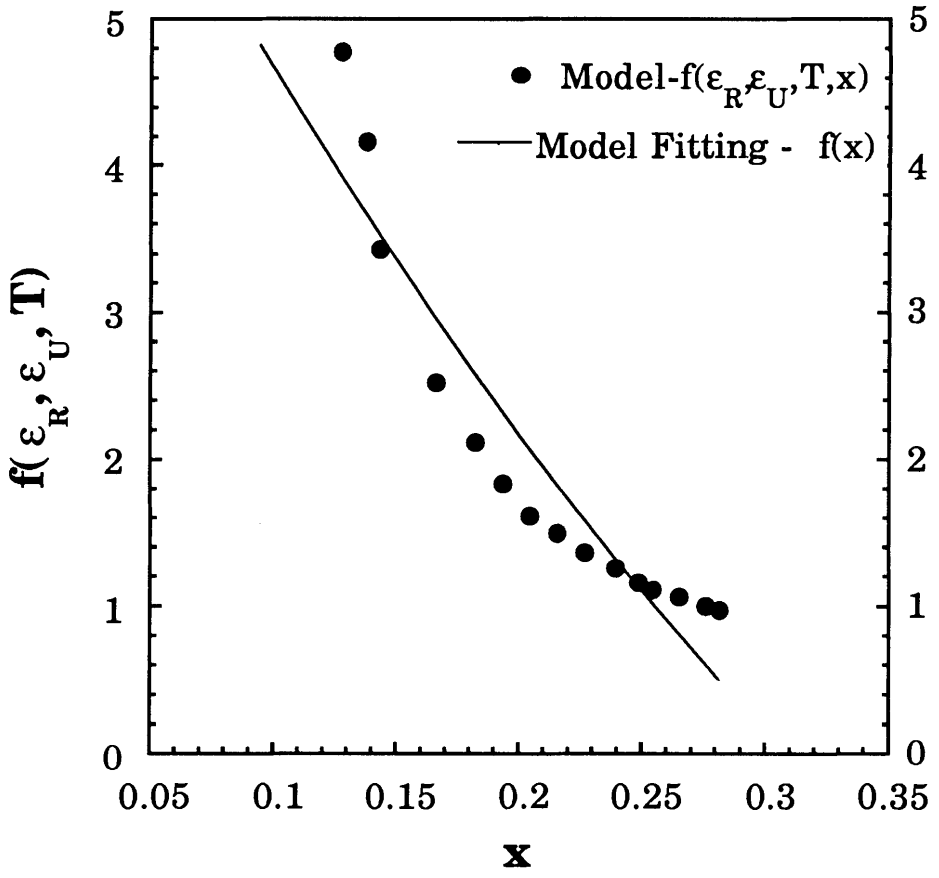

Figure 4.8: Model testing for imidization at 130°C

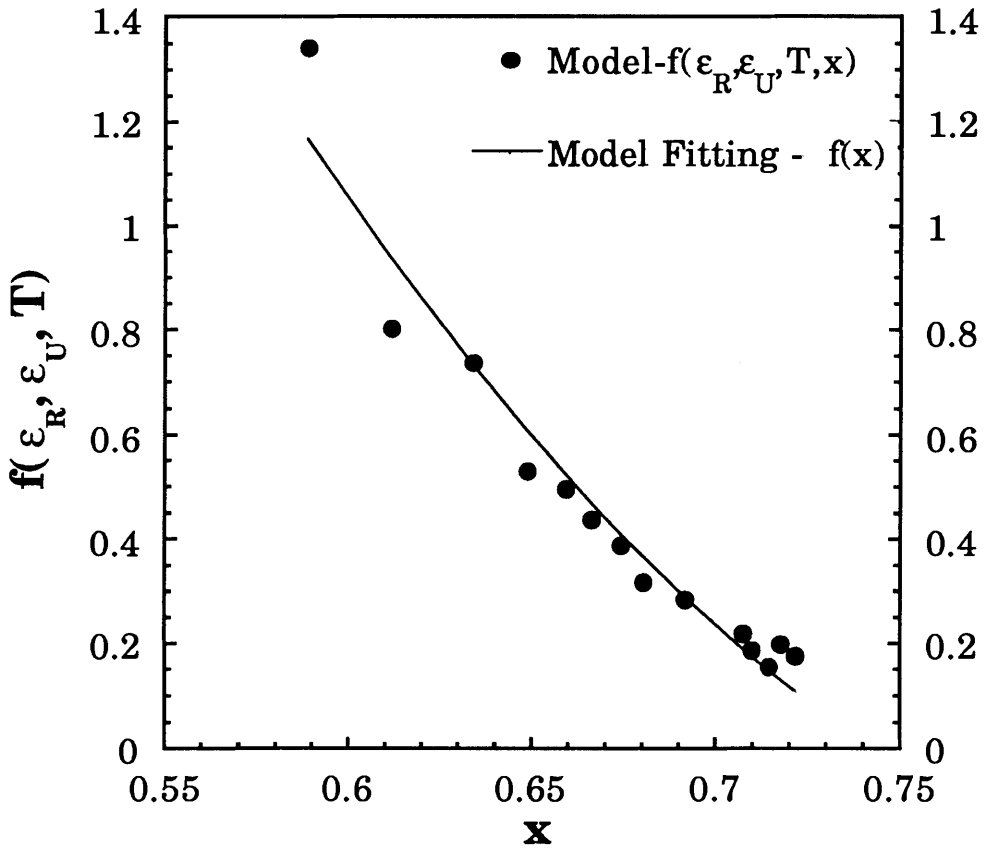

Figure 4.9: Model testing for imidization at 160°C

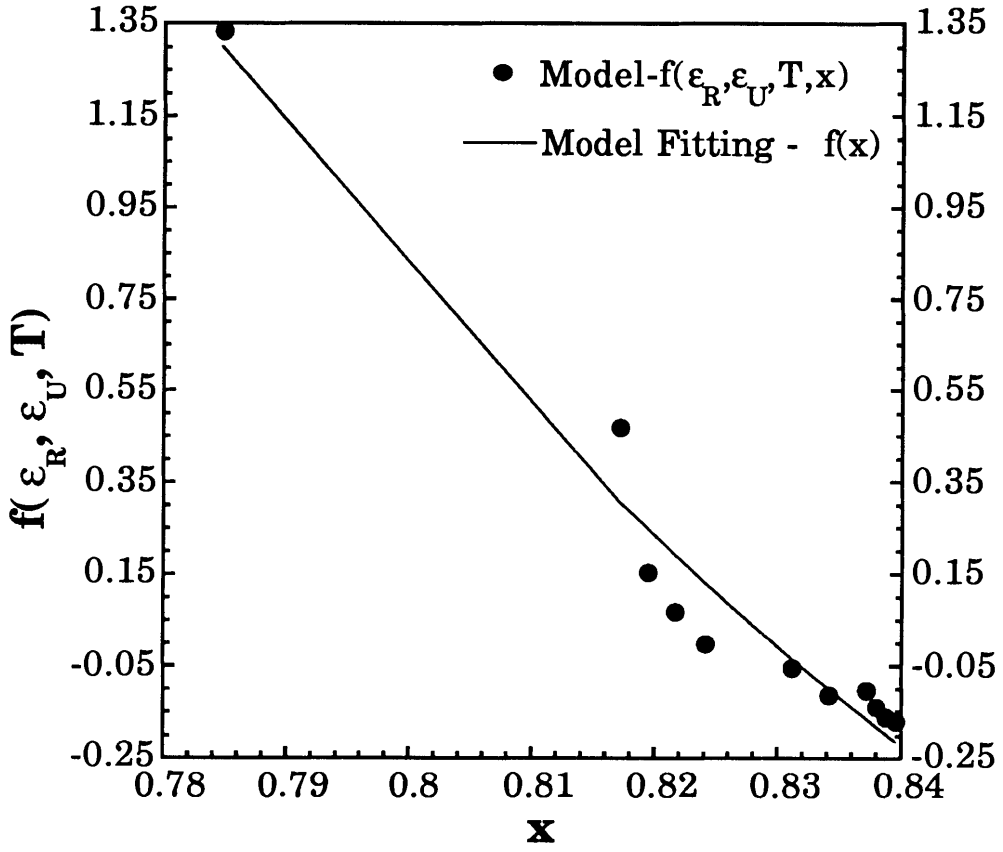

Figure 4.10: Model testing for imidization at 200°C

range of the extent of reaction covered at 130°C is greater, there could be a significant variation in the dipole moment of the amic acid unit because the average number of NMP molecules complexed to each unit changes significantly during the reaction. At the higher temperatures the average dipole moment of an amic acid unit does not vary significantly because the imidization range considered is smaller.

(2) Electrode Polarization:

The values of the left hand side of equation 4.41 early in the reaction could be higher than what they should be because the effect of electrode polarization has not been accounted for completely. Though electrode polarization might not be more dominant than the dipole orientation, it might still be having a significant effect on the measured permittivity. This could be because, in spite of being less than the permittivity, the conductivity contribution to the loss factor is of the same order of magnitude.

(3) Determination of ε_R:

One more reason why the model does not fit the data well could lie in the determination of ε_R. The determination of ε_R depends on the values obtained for the contribution of dipole orientation losses to the overall loss factor. A small error in the value obtained for conductivity could significantly affect the ionic conductivity contribution to the loss factor. As can be seen from the appendix, the values of τ_d and β do not follow any trend during the imidization. A better understanding of these parameters is needed. These parameters are significantly affected by the values of frequency of maximum loss and the maximum loss due to dipole orientation. A small difference in the ionic conductivity value used can change these two numbers significantly. However, taking data at lower frequencies might not

give a more accurate value for the conductivity, because electrode polarization affects dielectric data at lower frequencies.

In equation 4.41, the dipole moments are expressed in debye (D). The best fit of the model parameters, $g'_{r-11}\,\mathbf{p}_1^2$ and $g'_{r-12}\,\mathbf{p}_1$, was obtained at each of the three temperatures. These values are listed in table 4.2. It is necessary to determine the contributions of g'_{r-11}, g'_{r-12} and $\mathbf{p}_1$ in the fitted parameter ensembles to better understand the molecular behavior. One method to determine $\mathbf{p}_1$ is to estimate the highest possible dipole moment of an amic acid unit complexed with NMP. In order to determine the highest possible dipole moment in an amic acid unit, it is necessary to consider all the polar groups in an amic acid - 2 NMP complex unit. The dipole moment of the unit is the vector sum of moments of all the dipoles present. The highest moment that is possible is the scalar sum of the moments of all the polar units present:

(1)	1 diphenyl ether group:	dipole moment =	1 D [Smyth, 1930]
(2)	2 NMP molecules:	dipole moment =	8.26 D [M-PYROL, 1972]
(3)	2 benzoic acid groups:	dipole moment =	1.6 D [CRC,1986]
(4)	2 benzamide groups :	dipole moment =	7.2 D [CRC, !986]

Therefore, the highest possible dipole moment is about 18.5 D. The actual dipole moment should be lower than 18.5 D because some of the dipoles might cancel out. However, in absence of any information on the steric conformation of the unit, the dipole moment is taken as 18.5 D.

The parameter $g'_{r-11}\,\mathbf{p}_1^2$ increases with increase in temperature. However, if the value of $\mathbf{p}_1$ is about 18.5 D, then from the magnitudes of the ensemble the value of g'_{r-11} lies between 0 and 1. Considering equation 4.27-a, it can be inferred that the mean of the cosine of the angle between two amic acid units is negative, i.e. two amic acid dipoles preferentially lie anti-parallel to each other. With increase in temperature, the value of $\overline{\cos\,\gamma}$

becomes less negative. This implies that the increase in temperature makes the system more random. The randomness in the system increases with increase in temperature. The alignment of the dipoles is thus improved when the electric field is applied. This behavior is to be expected because, in terms of energy, two dipoles are most stable if they lie anti-parallel to each other. Steric hindrances tend to prevent the dipoles from being exactly anti-parallel. Thermal energy will tend to randomize the orientation, and if the temperature is high enough, then the dipoles might even subtend an acute angle.

It should be noted that if a dipole moment of an amic acid-NMP unit is taken to be as low as 4 D, the fitted parameter g'_{r-11} will lie in the range of 0 to 10. These values of g'_{r-11} are still reasonable in terms of the molecular interactions explained above in the preceding paragraph.

It is observed that the parameter $g'_{r-12}\,\mathbf{p}_1$ is negative. This means that the cosine of the angle between an amic acid unit and an imide unit is negative which indicates that the angle is an obtuse angle. This is to be expected due to reasons similar to those described above for two dipoles of amic acid units. From the magnitudes of the fitted parameter ensemble, it is observed that after putting $\mathbf{p}_1$ to be about 18.5 D, the interaction parameter lies between 0 and -1, which is in the expected range. However, no trend can be inferred in the variation of this parameter with temperature. Hence, relative to each other, the interaction of the dipoles does not seem to show any trend, in the presence of an electric field. It is difficult to determine the cause of this behavior. It could be because of the failure of the model to accurately describe the behavior of the system. Another possible reason could be that more values of g'_{r-12} are required as a function of temperature in order to confidently interpret the values of the interaction parameter in terms of molecular behavior.

The fitted parameters $g'_{r-11}\,\mathbf{p}_1^2$ and $g'_{r-12}\,\mathbf{p}_1$ lie in the range within which their magnitudes can be physically explained. However, understanding the trend in the

parameter $g'_{r-12}\,p_1$ requires further study. Another aspect that requires further consideration is the modification of the model to incorporate the variation of the dipole moment of an amic acid-NMP complex unit during imidization.

Table 4.2: Relationship between fitted parameters and temperature

T°C	$g'_{r-11}\,p_1^2$	$g'_{r-12}\,p_1$
130	7.6698	-8.5378
160	13.6881	-2.3705
200	112.0245	-11.3322

4.3 Ionic Conductivity and Extent of Imidization.

The starting material, Du Pont PI-2542 (PMDA-ODA polyamic acid in NMP) contains ionic impurities including Na^+, K^+, Cl^-, Li^+, etc. The total concentration of ionic species is of the order of 2.5 ppm [Du Pont, 1989]. After the pre-bake, when most of the unbound solvent is evaporated off, the concentration of the ionic species increases five-fold. This is because, while the ionic content does not change, the overall weight decreases by about 80%. Hence, at the onset of imidization, the concentration of ionic species is about 10-15 ppm.

Ionic conductivity is extracted as described in section 4.2-1. Figure 4.11 shows the variation of ionic conductivity with time of imidization at 130°C, 160°C and 200°C. Figure 4.12 shows the change in ionic conductivity as a function of extent of imidization. A

decrease is observed as the extent of imidization progresses. This is due to the decrease in mobility of the ionic species as the material becomes more closely packed because of imidization. It is to be noted that the concentration of the ionic species increases due to weight loss during imidization, but the drop in mobility plays a more dominant role in the change in ionic conductivity.

The curve at 130°C shows a smooth variation of conductivity with extent of reaction. However, at higher temperatures, scatter is observed in the data. The discrepancy in the shapes of the curves at 160°C and 200°C in figure 4.12 from the curve at 130°C is not properly understood.

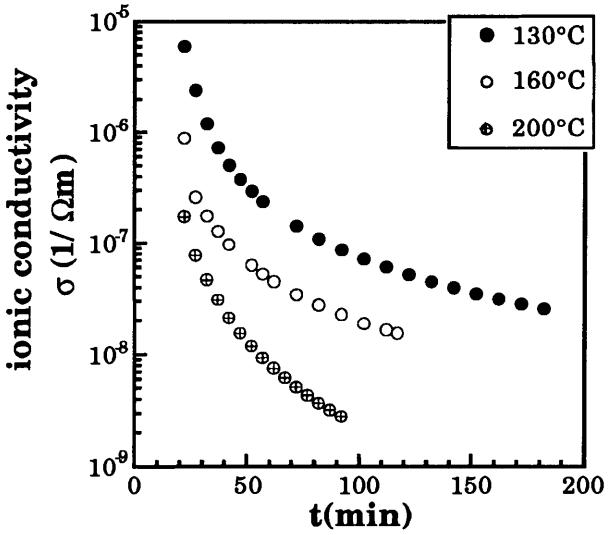

Figure 4.10: Variation of ionic conductivity during the imidization of polyamic acid to polyimide at 130°C, 160°C and 200°C.

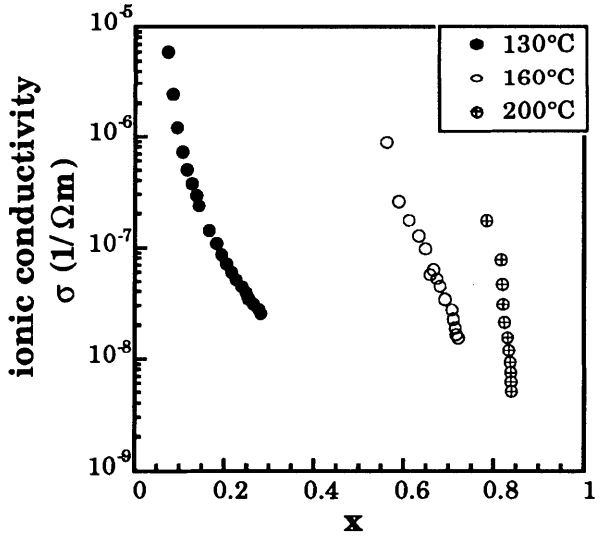

Figure 4.12: Ionic conductivity as a function of extent of reaction at 130°C, 160°C and 200°C

CHAPTER V.

CONCLUSIONS AND RECOMMENDATIONS

5.1 Summary and Conclusions

The imidization of PMDA-ODA polyamic acid was successfully monitored simultaneously using FT-IR spectroscopy and microdielectrometry. The method employed was to treat two samples to an identical pre-bake schedule. Subsequently, the imidization of each of those two samples was monitored separately using the two techniques, ensuring that the heating schedule was identical for both of them. Thus dielectric properties were obtained as a function of the extent of imidization.

From the FT-IR spectroscopic studies of isothermal imidization, it was observed that the imidization reaction started at a high rate and slowed down significantly. The final value of the extent of imidization increased with increase in the imidization temperature. This was true for imidization in air up to 350°C. At 130°C, the extent of reaction after 3 hours was about 28%. The imidization had not stopped completely even after proceeding for 3 hours at 130°C. At 160°C, the reaction had slowed down significantly after reaching about 73% completion in 2 hours. At 200°C, the reaction had almost come to a halt at 84% completion after about 60 minutes. At 350°C, the extent of reaction was the highest corresponding to an imide absorbance to aromatic absorbance ratio of 0.624. This value was assumed to correspond to 100% completion.

The monitoring of imidization using dielectrometry resulted in a final permittivity of about 5 after 3 hours at 130°C, about 3.8 after 2 hours at 160°C and about 3.3 after one hour at 200°C.

Dielectric measurements were also carried out on commercially available Kapton® film using the parallel plate measurement option of the dielectrometer. Raising the temperature decreased the permittivity. This behavior is counter-intuitive and was attributed to the decrease in the moisture content of the film due to rise in temperature. Since the molecular arrangement in Kapton is rigid, the dipole mobility is highly restricted. Hence the variation in permittivity over a large frequency range was very small. This prevented the accurate determination of the interaction parameter g'_{r-22}. However, the values that were determined lay in the expected range.

It was observed that the extent of imidization bears a strong relation to the change in dielectric properties. In the present investigation, the focus was on the permittivity. It has been recognized that the permittivity of a polar material depends on the dipole moment of the material. This dipole moment depends on the molecular structure, i.e. the chemistry. Change in the chemistry caused by the imidization reaction causes a change in permittivity. Based on this premise, modelling the effect of reaction on the dielectric permittivity of the material was attempted.

The model fit was fair at 160°C and 200°C. However, the data at 130°C shows a greater curvature than the model fit. Of the fitted parameters, $g'_{r-11}\,\mathbf{p}_1^2$ shows a trend that can be explained based on its physical significance. This is done by assuming a dipole moment of about 18.5 D for an amic acid unit complexed with 2 NMP molecules. The second fitted parameter, $g'_{r-12}\,\mathbf{p}_1$, whose values lie in the expected range, does not show a trend that can be effectively interpreted.

5.2 Recommendations for future work

Electrode polarization significantly affects data in the earlier part of the reaction. In order to obtain more dielectric data as a function of reaction, it is necessary to obtain useful dielectric data earlier in the reaction, when large increases occur in the extent of reaction as well as in the dielectric properties. Since FT-IR spectroscopic measurements as well as the frequency scans for dielectric measurements can be made very rapidly, it might be advantageous to run a high conductivity sensor and a low conductivity sensor simultaneously on one sample. Since, conductivity does dominate the loss factor at low frequencies, the high conductivity sensor might give an accurate measure of the relaxed permittivity.

The dipole moment of an amic acid-NMP unit changes during imidization due to the change in the number of NMP molecules complexed with each amic acid unit. It is necessary to incorporate this variation in the dipole moment in the model to relate the change in molecular structure to the dielectric properties.

The dielectric measurements performed on Kapton® film need to be made over a larger frequency range. The use of a network analyzer to perform high frequency measurements (frequencies greater than 100 kHz) is recommended. However, it must be noted that if the frequencies required to determine the unrelaxed permittivity is very high (of the order of GHz), then it might not be possible to determine ε_U. This is because electronic and atomic orientations are frequency dependant at those frequencies. Another aspect that needs further study is determining whether or not moisture causes the anomalous results in the permittivity measurements of fully imidized polyimide. This could be done by considering a pre-dried film and carrying out the experiments in a dry atmosphere.

The Kapton® film being used is not an electronic grade material. A parallel plate capacitor with a pure polyimide film dielectric can be obtained by depositing aluminium on a silicon wafer, spin-coating the electronic grade PI-2542 polyamic acid solution from Du Pont on the wafer, baking it at temperature of 350°C to 400°C and depositing another layer of aluminium on top. This film would be a better standard for fully imidized polyimide than the commercially available Kapton®.

The fitted parameters in the model are ensembles which need to be separated for a better understanding of the molecular behavior. To that end, it is necessary to determine the spatial arrangement of the various atoms in a polymer molecule. The large number of degrees of freedom in a polymer molecule effectively make the task extremely difficult. If one considers a monomer unit, it might be possible to determine the spatial structure and the dipole moment based on this structure. This dipole moment can be determined by considering the vector sum of all the dipole segments in the unit. The dipole moment thus depends on the conformation. The probability of a conformation depends on the energy of the conformation and is given by the Boltzman's distribution. Hence, the dipole moment of a unit is determined by considering all the spatial conformations, weighed by their probability. The angle between interacting units which can be similarly determined as described in section 4.1. This approach and the methods to determine energies of conformation have been described by Flory (1989). Attempts to compute the exact conformations and the conformational energies are in progress by other workers [Lazaridis et al., 1991].

REFERENCES

Chemical Company, Inc., Catalog Handbook of Fine Chemicals, Milwaukee, WI (1990).

Berry, G.C. and Fox, T.G., *Advances in Polymer Science*, **5**, 261 (1968).

Bidstrup, S.A., Sheppard, N.F., and Senturia, S.D., *Polymer Engineering and Science*, **29**, 325 (1989).

Bidstrup, W. W., Bidstrup, S. A., and Senturia, S.D., *Proceedings, 46th Annual Technical Conference,* Society of Plastics Engineers, **34**, 960 (1988).

Brekner, M.J., and Feger, C., *Journal of Polymer Science: Part A Polymer Chemistry*, **25**, 2479 (1987).

Brown, G.A., in "Polymers for Electronic Applications", E.D. Feit and C.Wilkins, Jr. (eds.), ACS Symposium Series **184**, American Chemical Society, Washington, D.C., 151 (1982).

CRC Handbook of Chemistry and Physics, Weast, R.C. (ed.), 67th ed. CRC Press, Inc., Boca Raton (1986).

Cole, K.S. and Cole, R.H., *Journal of Chemical Physics*, **9**, 341 (1941).

Davidson, D.W. and Cole, R.H., *Journal of Chemical Physics*, **18**, 1417 (1950).

Day, D.R., *Polymer Engineering and Science*, **29**, 334 (1989).

Day, D.R., and Senturia, S.D., in "Polyimides: Synthesis, Characterization and Applications" K. L. Mittal (ed.), Plenum Press, New York, 249 (1982).

Debye, P., "Polar Molecules", The Chemical Catalog Company (1929).

Du Pont Company, Electronics Department, Kapton Polyimide Film:Summary of Properties, Wilmington, DE (1988).

Du Pont Company, Electronics Department, PI-2542D, Material Data Sheet, Wilmington, DE (1989).

Feger, C., *Proceedings, 45th Annual Technical Conference,* Society of Plastics Engineers, **33**, 967 (1987).

Feger, C., *Polymer Engineering and Science*, **29**, 347 (1989).

Frölich, H., "Theory of Dielectrics: Dielectric Constant and Dielectric Loss", Oxford University Press (1958).

Geldermans, P., Goldsmith, C. and Bedetti, F., in "Polyimides: Synthesis, Characterization and Applications", K. L. Mittal (ed.), Plenum Press, New York, 695 (1982).

Holmes, B.S. and Trask, C.A., *Journal of Applied Polymer Science*, **35**, 1399 (1988).

Iida, K., Waki, M., Nakamura, S., Ieda, M. and Sawa, G., *Japanese Journal of Applied Physics*, **23**, 1573 (1984).

Ito, Y., Masayuki, H., Kimura, T. and Mizutani, T., *Japanese Journal of Applied Physics*, **29**, 1128 (1990).

Jensen, R.J. and Lai, J.H., in "Polymers for Electronic Applications", J.H. Lai (ed.), CRC Press (1989).

Kienle, R.H. and Race, H.H., *Transactions Electrochemical Society*, **65**, 87 (1934).

Kirkwood, J.G., *Journal of Chemical Physics*, **7**, 911 (1939).

Kranbuehl, D.E., Delos, S.E., Jue, P.K. and Schellenberg, R.K., in "Polyimides: Synthesis, Characterization and Applications" K. L. Mittal (ed.), Plenum Press, New York, 207 (1982).

Kranbuehl, D.E. et al., *ACS Symposium Series No. 367: Cross-Linked Polymers*, 100 (1988).

Laius, L. A., Bessonov, M. I., Kallistova, Y. V., Adrova, N. A., Florinskii, F. S., *Polymer Science USSR*, **9A**, 2470 (1967).

Laius, L. A. and Tsapovetsky, M.I., in "Polyimides: Synthesis, Characterization and Applications", K. L. Mittal (ed.), Plenum Press, New York, 295 (1982).

Lazaridis, T., Tobias, D. J., Brooks, C. L., Paulatis, M. E., *Journal of Chemical Physics*, **95**, 7612 (1991).

Lindsey, C.P. and Patterson, G.D., *Journal of Chemical Physics*, **73**, 3348 (1980).

M-PYROL® N-Methyl-2-Pyrrolidone Handbook, GAF Corporation Chemical Division, New York, 1972.

McCrum, N.G., Read, B.E. and Williams, G., "Anelastic and Dielectric Effects in Polymeric Solids", John Wiley and Sons (1967).

Micromet Instruments, Inc., *Principles of Dielectrometry.*

Micromet Instruments, Inc., Users Guide to Eumetric System II Microdielectrometer, Cambridge, MA (1985).

Montroll, E.W. and Bendler, J.T., *Journal Statistical Physics*, **34**, 129 (1984).

Nass, K.A. and Seferis, J.C., *Polymer Engineering and Science*, **29**, 315 (1989).

Navarre, M., in "Polyimides: Synthesis, Characterization and Applications", K. L. Mittal (ed.), Plenum Press, New York, 429 (1982).

Onsager, L., *Journal of the American Chemical Society*, **58**, 1486 (1936).

Osredkar, R., *Microelectronics Reliability*, **28**, 599 (1988).

Palmese, G.R. and Gillham, J.K., *Journal of Applied Polymer Science*, **34**, 1925 (1987).

Pryde, C.A., *Journal of Polymer Science: Part A Polymer Chemistry*, **27**, 711 (1989-a).

Pryde, C.A., in "Polymeric Materials for Electronics Packaging and Interconnection", J.H. Lupinski and R.S. Moore (eds.), American Chemical Society, 57 (1989-b).

Pryde, C.A., *Proceedings, 48th Annual Technical Conference,* Society of Plastics Engineers, **36**, 439 (1990).

Senturia, S.D. and Sheppard, N.F., *Advances in Polymer Science*, **80**, 1 (1986).

Sheppard, D.D., Lee, H.L., Day, D.R., *Proceedings 34th International SAMPE Symposium*, Society for the Advancement of Materials and Process Engineering, 407 (1989).

Sheppard, N.F., "Dielectric Analysis of the Cure of Thermosetting Epoxy/Amine Systems", Ph. D. Thesis, Massachusetts Institute of Technology (1986).

Shlesinger, M.F., *Journal Statistical Physics*, **36**, 639 (1984).

Simoff D.A., Pryde, C.A., Johnson, E.T. and Robinson, M.B., *Proceedings, 48th Annual Technical Conference,* Society of Plastics Engineers, **36**, 960 (1990).

Simpson, J.O., "Modelling Viscosity and Ionic Conductivity of Epoxy Resins using Free Volume Concepts", M.S. Thesis, Georgia Institute of Technology, (1989).

Smyth, C.P.,"Dielectric Constant and Molecular Structure", The Chemical Catalog Company (1931).

Snyder, R.W. and Painter, P.C., in "Polymeric Materials for Electronics Packaging and Interconnection", J.H. Lupinski and R.S. Moore (eds.), American Chemical Society, 49 (1989).

Snyder, R.W., Sheen, C.W. and Painter, P.C., *Applied Spectroscopy*, **42**, 503 (1988).

Soane, D.S. and Martynenko, Z.M., "Polymers in Microelectronics", Elsevier, 153-206 (1989).

Solymar, L. and Walsh, D.,"Lectures on the Electrical Properties of Materials", Oxford University Press, 262-289 (1988).

Sze, S.E., in "VLSI Technology", McGraw Hill, New York (1983).

Tessier, T.G., Adema, G.M. and Turlik, I., *Proceedings Electronic Component Conference*, IEEE, 127 (1989).

Wachsman, E.D. and Frank, C.W., *Polymer*, **29**, 1191 (1988).

Williams, G. and Watts, D.C., *Transactions Faraday Society*, **66**, 80 (1970).

Williams, G., Watts, D.C., Dev, S.B. and North, A.M., *Transactions Faraday Society*, **67**, 1397 (1971)

Wilson, A.M., *Thin Solid Films*, **83**, 145 (1981).

Wilson, A.M., Laks, D. and Davis, S.M., in "Polymers for Electronic Applications", E.D. Feit and C.Wilkins, Jr. (eds.), ACS Symposium Series **184**, American Chemical Society, Washington, D.C., 107 (1982).

APPENDIX

(Data Summary)

Data Analysis of Imidization at 130°C

t(min)	ε''_{max}	$\varepsilon'(\varepsilon''_{max})$	$f(\varepsilon''_{max})$ (Hz)	τ_d (ms)	β	ε_U	$\varepsilon_R-\varepsilon_U$	ε_R	σ (1 / Ωm)	x	LHS (eqn 4.41)	RHS (eqn 4.41)
47	1.3815	7.7252	1000	0.2588	0.5408	5.4787	3.5	8.9787	3.733E-07	0.1278	4.7787	3.9312
52	1.144	7.2749	1000	0.2625	0.5314	5.3882	2.9543	8.3425	2.921E-07	0.1381	4.1608	3.6651
57	0.8779	6.8585	1000	0.2788	0.4929	5.3204	2.3571	7.6775	2.367E-07	0.1435	3.4288	3.529
72	0.5907	6.2512	1000	0.2964	0.4571	5.1511	1.6405	6.7916	1.425E-07	0.1665	2.5214	2.9594
82	0.4697	5.9738	1000	0.3093	0.4337	5.0609	1.3418	6.4027	1.092E-07	0.1826	2.1159	2.5763
92	0.3945	5.7648	1000	0.3152	0.4239	4.9836	1.134	6.1176	8.622E-08	0.1938	1.829	2.3176
102	0.3371	5.5981	1000	0.3186	0.4183	4.9233	0.9842	5.9075	7.123E-08	0.2048	1.6127	2.0692
112	0.3017	5.482	1000	0.3319	0.3979	4.8528	0.8982	5.751	6.008E-08	0.216	1.4956	1.8233
122	0.2748	5.3783	1000	0.3291	0.402	4.81	0.8125	5.6225	5.139E-08	0.2272	1.3639	1.5816
132	0.2514	5.277	1000	0.3226	0.412	4.7674	0.745	5.5124	4.436E-08	0.2397	1.2586	1.321
142	0.232	5.2098	1000	0.323	0.4113	4.7389	0.6835	5.4224	3.913E-08	0.2488	1.1597	1.1372
152	0.2215	5.1422	1000	0.3172	0.4206	4.7008	0.6476	5.3484	3.451E-08	0.2547	1.1079	1.0194
162	0.2062	5.0833	1000	0.3276	0.4043	4.6589	0.6151	5.274	3.087E-08	0.2655	1.0583	0.8079
172	0.1933	5.033	1000	0.333	0.3964	4.6286	0.5776	5.2062	2.791E-08	0.2764	0.9959	0.6011
182	0.1888	4.9868	1000	0.3278	0.404	4.5979	0.5593	5.1572	2.531E-08	0.2819	0.9698	0.4983

Data Analysis of Imidization at 160°C

t(min)	ε''_{max}	$\varepsilon'(\varepsilon''_{max})$	$f(\varepsilon''_{max})$ (Hz)	τ_d (ms)	β	ε_U	$\varepsilon_R-\varepsilon_U$	ε_R	σ (1 / Ωm)	x	LHS (eqn 4.41)	RHS (eqn 4.41)
27	0.15	5.2559	2000	0.5005	0.1116	4.3125	0.8504	5.1629	2.587E-07	0.5890	1.3410	1.1650
32	0.1218	4.6455	3000	0.182	0.2204	4.2277	0.5253	4.753	1.751E-07	0.6119	0.8015	0.9360
37	0.1078	4.5107	2000	0.2591	0.2341	4.1597	0.4886	4.6483	1.274E-07	0.6342	0.7370	0.7316
42	0.102	4.343	5000	0.0731	0.3537	4.1086	0.371	4.4796	9.716E-08	0.6489	0.5288	0.6073
52	0.0901	4.2399	4000	0.0934	0.3449	4.0286	0.3188	4.3474	6.302E-08	0.6664	0.4367	0.4690
62	0.078	4.1277	5000	0.0644	0.4129	3.9699	0.2537	4.2236	4.476E-08	0.6805	0.3157	0.3667
72	0.0696	4.0749	4000	0.0884	0.3686	3.9203	0.237	4.1573	3.393E-08	0.6918	0.2836	0.2893
82	0.0616	4.0163	4000	0.0861	0.3804	3.883	0.2062	4.0892	2.726E-08	0.7076	0.2187	0.1893
92	0.0592	3.9688	4000	0.0803	0.4143	3.8493	0.188	4.0373	2.255E-08	0.7100	0.1863	0.1750
102	0.0518	3.927	4000	0.0838	0.3934	3.8179	0.1715	3.9894	1.879E-08	0.7146	0.1546	0.1483
112	0.0485	3.9103	2000	0.1998	0.318	3.7886	0.1928	3.9814	1.64E-08	0.7177	0.1981	0.1306

Data Analysis of Imidization at 200°C

t(min)	ε''_{max}	$\varepsilon'(\varepsilon''_{max})$	$f(\varepsilon''_{max})$ (Hz)	τ_d (ms)	β	ε_U	$\varepsilon_R-\varepsilon_U$	ε_R	σ (1 / Ωm)	x	LHS (eqn 4.41)	RHS (eqn 4.41)
22	0.2552	4.3202	1000	0.4247	0.2958	3.6392	0.7748	4.414	1.728E-06	0.7848	1.334	1.299
27	0.0949	3.8471	1000	0.5563	0.2157	3.5154	0.3624	3.8778	7.734E-07	0.8172	0.468	0.307
32	0.0469	3.5965	3000	0.186	0.2149	3.4321	0.216	3.6481	4.635E-07	0.8195	0.154	0.248
37	0.0396	3.5047	3000	0.1783	0.2256	3.3716	0.1762	3.5478	3.065E-07	0.8217	0.068	0.191
42	0.033	3.4344	3000	0.1754	0.23	3.3253	0.1457	3.471	2.118E-07	0.8242	-0.002	0.129
47	0.0302	3.3792	3000	0.1581	0.2596	3.2892	0.1253	3.4145	1.545E-07	0.8312	-0.054	-0.036
52	0.0252	3.3228	5000	0.0841	0.2992	3.2562	0.1015	3.3577	1.19E-07	0.8342	-0.113	-0.102
57	0.0251	3.3111	2000	0.2587	0.2345	3.2295	0.1053	3.3348	9.303E-08	0.8372	-0.104	-0.166
62	0.021	3.2644	3000	0.1538	0.2681	3.2035	0.0905	3.294	7.506E-08	0.838	-0.140	-0.182
67	0.0195	3.2399	3000	0.1524	0.2712	3.1839	0.0819	3.2658	6.188E-08	0.8388	-0.162	-0.199
72	0.0175	3.2152	3000	0.1595	0.257	3.1626	0.0779	3.2405	5.105E-08	0.8396	-0.171	-0.214